

# Arabidopsis glutathione reductase 2 is indispensable in plastids, while mitochondrial glutathione is safeguarded by additional reduction and transport systems

Laurent Marty<sup>1</sup>, Daniela Bausewein<sup>1,2</sup>, Christopher Müller<sup>1</sup>, Sajid Ali Khan Bangash<sup>2</sup> , Anna Moseler<sup>2</sup> , Markus Schwarzländer<sup>3</sup> , Stefanie J. Müller-Schüssele<sup>2</sup> , Bernd Zechmann<sup>4</sup>, Christophe Riondet<sup>5,6</sup>, Janneke Balk<sup>7</sup> , Markus Wirtz<sup>1</sup> , Rüdiger Hell<sup>1</sup> , Jean-Philippe Reichheld<sup>5,6</sup> and Andreas J. Meyer<sup>2</sup> 

<sup>1</sup>Centre for Organismal Studies, Heidelberg University, Im Neuenheimer Feld, 360, D-69120, Heidelberg, Germany; <sup>2</sup>Institute of Crop Science and Resource Conservation (INRES), University of Bonn, Friedrich-Ebert-Allee 144, D-53113, Bonn, Germany; <sup>3</sup>Institute for Biology and Biotechnology of Plants, University of Münster, Schlossplatz 8, D-48143, Münster, Germany; <sup>4</sup>Center of Microscopy and Imaging, Baylor University, One Bear Place 97046, Waco, TX 76798-7046, USA; <sup>5</sup>Laboratoire Génome et Développement des Plantes, Université de Perpignan, Via Domitia, F-66860, Perpignan, France; <sup>6</sup>Laboratoire Génome et Développement des Plantes, CNRS, F-66860, Perpignan, France; <sup>7</sup>John Innes Centre and University of East Anglia, Norwich Research Park, Norwich, NR4 7UH, UK

## Summary

Author for correspondence:

Andreas Meyer

Tel: +49 228 73 60353

Email: andreas.meyer@uni-bonn.de

Received: 18 April 2019

Accepted: 23 July 2019

New Phytologist (2019)

doi: 10.1111/nph.16086

**Key words:** ABCB25, dual targeting, embryo lethality, glutathione redox status, glutathione reductase 2, mitochondria, NTR, redox-sensitive GFP.

- A highly negative glutathione redox potential ( $E_{\text{GSH}}$ ) is maintained in the cytosol, plastids and mitochondria of plant cells to support fundamental processes, including antioxidant defence, redox regulation and iron–sulfur cluster biogenesis. Out of two glutathione reductase (GR) proteins in Arabidopsis, GR2 is predicted to be dual-targeted to plastids and mitochondria, but its differential roles in these organelles remain unclear.
- We dissected the role of GR2 in organelle glutathione redox homeostasis and plant development using a combination of genetic complementation and stacked mutants, biochemical activity studies, immunogold labelling and *in vivo* biosensing.
- Our data demonstrate that GR2 is dual-targeted to plastids and mitochondria, but embryo lethality of *gr2* null mutants is caused specifically in plastids. Whereas lack of mitochondrial GR2 leads to a partially oxidised glutathione pool in the matrix, the ATP-binding cassette (ABC) transporter ATM3 and the mitochondrial thioredoxin system provide functional backup and maintain plant viability.
- We identify GR2 as essential in the plastid stroma, where it counters GSSG accumulation and developmental arrest. By contrast a functional triad of GR2, ATM3 and the thioredoxin system in the mitochondria provides resilience to excessive glutathione oxidation.

## Introduction

The use of oxygen by aerobic organisms allows them to obtain more energy from carbohydrates, by accessing a larger reduction potential difference. Other metabolic reactions in the cell, however, also lead to reduction of oxygen and give rise to reactive oxygen species (ROS), such as superoxide ( $\text{O}_2^-$ ), hydrogen peroxide ( $\text{H}_2\text{O}_2$ ) and hydroxyl radicals. Low levels of ROS have been implicated in signalling between subcellular compartments as well as long-distance signalling regulating plant development and metabolism (Foyer & Noctor, 2009; Gilroy *et al.*, 2016). However, at higher concentrations, ROS may oxidise lipids, proteins and DNA and render these molecules nonfunctional. Therefore, ROS constitute a major threat to the cell and need to be tightly controlled. Cellular compartments that can be particularly affected by oxidative stress include the plastids, mitochondria and peroxisomes (Mittler *et al.*, 2004). In chloroplasts, the

Mehler reaction and antenna pigments are major sources of  $\text{O}_2^-$  formation (Asada, 1999). In mitochondria, overreduction of the electron transport chain results in  $\text{O}_2^-$  production at complexes I and III (Moller, 2001). In both compartments,  $\text{O}_2^-$  quickly dismutates to  $\text{H}_2\text{O}_2$  and  $\text{O}_2$  in a reaction catalysed by superoxide dismutase (SOD).

In plants,  $\text{H}_2\text{O}_2$  produced by SODs is further reduced to water by peroxidases such as ascorbate peroxidases (APXs), glutathione peroxidase-like enzymes (GPXLs) and peroxiredoxins (PRXs). While GPXLs and PRXs are dependent on thioredoxins (TRXs) as primary electron donor (Finkemeier *et al.*, 2005; Navrot *et al.*, 2006; Attacha *et al.*, 2017), APXs use electrons from ascorbate. The resulting dehydroascorbate is recycled through the ascorbate–glutathione cycle, which links  $\text{H}_2\text{O}_2$  detoxification to the redox dynamics of the glutathione redox couple.

Glutathione is the most abundant low-molecular-weight thiol redox buffer in all eukaryotic organisms and most Gram-negative

bacteria, including cyanobacteria and purple bacteria, and is present at millimolar concentrations (Fahey, 2001; Meyer *et al.*, 2001). After synthesis in plastids and the cytosol (Pasternak *et al.*, 2008; Maughan *et al.*, 2010), reduced glutathione (GSH) is transported throughout the cell to fulfil a broad range of functions in metabolism and detoxification of xenobiotics and H<sub>2</sub>O<sub>2</sub> (Meyer, 2008). Upon oxidation, two molecules of GSH convert to glutathione disulfide (GSSG). In the cytosol, mitochondria and plastids the glutathione redox potential ( $E_{\text{GSH}}$ ) is highly reduced with only nanomolar concentrations of GSSG present under non-stress conditions (Meyer *et al.*, 2007; Schwarzländer *et al.*, 2008). Such a high GSH/GSSG ratio is believed to be maintained by NADPH-dependent glutathione reductases (GRs). In contrast with bacteria, animals and yeast, plant genomes encode two GRs (Xu *et al.*, 2013). In Arabidopsis, GR1 is present in the cytosol, the nucleus and peroxisomes (Reumann *et al.*, 2007; Marty *et al.*, 2009; Delorme-Hinoux *et al.*, 2016). The second isoform, GR2, is dual-targeted to mitochondria and plastids (Creissen *et al.*, 1995; Chew *et al.*, 2003), as supported by proteomics analyses of purified organelles (Ito *et al.*, 2006; Peltier *et al.*, 2006). However, Yu *et al.* (2013) found no evidence for mitochondrial targeting of full-length GR2–YFP constructs and concluded exclusive plastidic localisation. While we found that Arabidopsis mutants lacking cytosolic GR1 are fully viable (Marty *et al.*, 2009), a deletion mutant lacking functional GR2 is embryo lethal (Tzafirir *et al.*, 2004; Bryant *et al.*, 2011; Ding *et al.*, 2016b). These observations raise important questions about the exact localisation of GR2, the cause of lethality in *gr2* mutants, and about the mechanisms maintaining a highly negative glutathione redox potential ( $E_{\text{GSH}}$ ) in plastids and mitochondria.

Viability of Arabidopsis mutants lacking cytosolic GR1 is maintained by the NADPH-dependent TRX system (NTS) (Marty *et al.*, 2009). In this case, electrons supplied by NADPH are transferred to GSSG via NADPH-dependent TRX reductase (NTR) and TRX. Arabidopsis contains two NTRs, NTRA and NTRB, which are both targeted to the cytosol, the nucleus and mitochondria (Reichheld *et al.*, 2005; Marchal *et al.*, 2014). In addition, plastids contain a remotely related bifunctional NTR, NTRC, which contains its own TRX domain (Serrato *et al.*, 2004). NTRC has been shown to be responsible for transferring electrons from NADPH to 2-Cys PRX for H<sub>2</sub>O<sub>2</sub> detoxification (Perez-Ruiz *et al.*, 2017) and for redox regulation of ADP-glucose pyrophosphorylase (Michalska *et al.*, 2009). While NTRC may be active in the dark and in heterotrophic tissues, classical non-fused plastidic TRXs are reduced by electrons from the photosynthetic electron transport chain via ferredoxin-dependent TRX reductase (FTR) which implies that they exercise their reductive capacity only in the light (Buchanan & Balmer, 2005). Whether and to what extent the different subcellular TRX systems contribute to organellar glutathione redox homeostasis is yet unknown.

Beyond maintenance of a highly negative  $E_{\text{GSH}}$  through continuous reduction of GSSG, ATP-driven sequestration of GSSG to the vacuole by ATP-binding cassette (ABC)-transporters has been shown to provide an overflow valve for high cytosolic GSSG amounts in yeast (Morgan *et al.*, 2013). Similarly, the ABC

transporter of the mitochondria Atm1 in yeast and its functional homologue ATM3 in Arabidopsis (systematic name ABCB25) transport GSSG, but not GSH, driven by ATP hydrolysis (Schaedler *et al.*, 2014). The ATPase domain of Atm1 is orientated towards the mitochondrial matrix (Leighton & Schatz, 1995), indicating that these proteins may export GSSG out of the mitochondria. In support of this, Arabidopsis *atm3* mutants were shown to have a more oxidised  $E_{\text{GSH}}$  in the mitochondrial matrix compared with wild-type (Schaedler *et al.*, 2014). However, the primary substrate of Atm1/ATM3 is thought to be GSH-bound persulfide for the biosynthesis of cytosolic iron-sulfur clusters (Kispal *et al.*, 1999; Srinivasan *et al.*, 2014). This raises the question of the ATM3's relative contribution to other systems in GSSG clearance of the mitochondrial matrix.

Here, we address the role of GR2 in glutathione redox homeostasis in mitochondria and plastids. We localise GR2 by immunogold labelling and complement the lethal *gr2* null mutant in a compartment-specific manner. Those analyses provide clear evidence for dual localisation of GR2 and for an essential role in plastids only. To address the question of why mitochondria are less affected than plastids by the lack of GR2, we focussed our attention on other possible mechanisms involved in maintaining the  $E_{\text{GSH}}$  in the matrix. Using a series of physiological and genetic analyses we identify the involvement of alternative GSSG reduction systems and of GSSG export in  $E_{\text{GSH}}$  maintenance in the mitochondrial matrix.

## Materials and Methods

The following procedures are described in Supporting Information Methods S1 and S2: Antibody production and gel blot analysis; Immunogold labelling and electron microscopy. Primers used in this work are given in Table S1.

### Plant material and growth conditions

The study was conducted with *Arabidopsis thaliana* ecotype Columbia-0 ([L.] Heynh.) as the wild-type control and the mutants *gr2-1* (SALK\_040170, (Alonso *et al.*, 2003), *emb2360-1* (Tzafirir *et al.*, 2004), *ntra ntrb* (Reichheld *et al.*, 2007), *rml1* (Vernoux *et al.*, 2000) and *gsh1-1* (Cairns *et al.*, 2006), *gr1-1* (Marty *et al.*, 2009), and *atm3-4* (Bernard *et al.*, 2009), all generated in the Col-0 background. Plants were grown under short-day conditions: 8 h light at 22°C and 16 h dark at 19°C and light intensity was set to 120 μmol photons m<sup>-2</sup> s<sup>-1</sup>. To induce flowering, plants were transferred to long-day conditions: 16 h light at 22°C and 8 h dark at 19°C, light intensity was 160 μmol photons m<sup>-2</sup> s<sup>-1</sup>.

To genotype wild-type and mutant plants, genomic DNA was extracted from the leaf tissue according to (Edwards *et al.*, 1991).

Seeds produced by a double heterozygous *gr2-1 rml1* plant were plated on phytagel as described before (Meyer & Fricker, 2000). For rescue experiments, the growth medium was supplemented with filter-sterilised GSH (Sigma-Aldrich) to a final concentration of 1 mM before gelling. Seedlings exhibiting a characteristic *rml1* phenotype after germination were transferred to GSH plates and further development was monitored for 12 d.

## Cloning and plant transformation

Standard molecular biology technologies like growth of bacteria, plasmid isolation and polymerase chain reaction (PCR) were applied according to (Sambrook *et al.*, 1989). For cloning, all DNA fragments were amplified by PCR and blunt-end subcloned into pCAP (Roche Applied Science, Mannheim, Germany) with primers listed in Table S1. Accuracy of the cloned fragment was verified by sequencing by SeqLab (Göttingen, Germany). Different signal peptides were ligated into the pBinAR vector (Höfgen & Willmitzer, 1990) to achieve compartment-specific complementation. The transketolase targeting peptide (TK<sub>TP</sub>) sequence was cloned into pBinAR as described before (Wirtz & Hell, 2003). Similarly, the serine hydroxymethyltransferase target peptide (SHMT<sub>TP</sub>) was amplified and cloned behind the 35S promoter of pBinAR using *KpnI* and *BamHI*. To verify targeting, both signal peptides were also fused to the N-terminus of roGFP. For compartment-specific complementation the GR2 sequence without its endogenous target peptide of 77 amino acids (aa) consistently determined by CHLOROP 1.1 (<http://www.cbs.dtu.dk/services/ChloroP/>) and SIGNALP 3.0 (<http://www.cbs.dtu.dk/service/s/SignalP/>) (Bendtsen *et al.*, 2004) was amplified from cDNA. Since the *gr2-1* mutants carried kanamycin resistance the constructs were transferred to the Basta<sup>®</sup> resistance vector pBarA (a gift from Sabine Zachgo) using *HindIII* and *EcoRI* restriction sites. For constructs with the endogenous GR2 promoter, 2.1 kb were amplified from genomic DNA and used to replace the 35S promoter in pBinAR with *EcoRI* and *KpnI*.

Plant transformation was carried out by floral dip (Clough and Bent, 1998). For selection of positive transformants 2-wk-old plants were sprayed with Basta<sup>®</sup> (200 mg l<sup>-1</sup> glufosinate ammonium; Bayer Crop Science, Monheim, Germany).

Arabidopsis plants were transformed with the vector pBinAR-SHMT<sub>TP</sub>-roGFP2-Grx1 as described earlier (Albrecht *et al.*, 2014). For both wild-type and plastid-complemented *gr2* mutants, lines with incomplete mitochondrial targeting of roGFP2-Grx1 were selected.

## Protein purification and mitochondrial isolation

For recombinant protein expression, the pET28a and pETG10a constructs were transformed in *E. coli* HMS174 cells. Cells were grown at 37°C to an OD<sub>600</sub> nm of 0.8 in selective medium containing 50 µg ml<sup>-1</sup> kanamycin for pET28a or 100 µg ml<sup>-1</sup> ampicillin for pETG10a. Protein purification was performed as reported before (Marty *et al.*, 2009). Mitochondria were isolated from 13- to 16-d-old hydroponic Arabidopsis seedling cultures as described previously (Sweetlove *et al.*, 2007).

## High-performance liquid chromatography (HPLC) measurement of low-molecular-weight thiols

Leaf material was harvested from 6-wk-old plants grown on soil under short-day conditions. Leaf tissue was snap frozen in liquid nitrogen, ground to fine powder and extracted. Extraction, derivatisation and quantification of low-molecular-weight thiols by HPLC were done as described before (Meyer *et al.*, 2007).

## Analysis of embryo development and pollen viability

Embryos, ovules or whole siliques were destained with Hoyer's solution (7.5 g gum arabic, 100 g chloral hydrate, 5 ml glycerol, 60 ml water) for at least 4 h. The embryos were analysed by differential interference contrast (DIC) microscopy with a Leica DM/RB microscope equipped with a DFC 320 camera (Leica Microsystems, Wetzlar, Germany). Pollen from mature flowers were stained according to Alexander (Alexander, 1969) and analysed by bright field microscopy.

## Chlorophyll fluorescence measurement

Chlorophyll fluorescence was recorded after dark adaptation for at least 30 min with a pulse-amplitude modulated (PAM) fluorimeter (Junior PAM, Walz, Effeltrich, Germany).  $F_v/F_m$  was calculated as a measure of the maximum potential quantum yield of photosystem II.

## Confocal laser scanning microscopy

Whole leaves of 3-wk-old Arabidopsis plants were placed in water on a slide and covered with a coverslip. Leaves were imaged on Zeiss confocal microscopes LSM510META or LSM780 (Carl Zeiss MicroImaging, Jena, Germany) equipped with lasers for 405- and 488-nm excitation. Images were collected with either a ×25 lens (Plan-Neofluar ×25/0.8 Imm corr, Zeiss) or a ×63 lens (C Apochromat ×63/1.2 W corr, Zeiss). For localisation studies GFP was excited at 488 nm and emission was collected with a 505–530 nm band-pass filter. Chlorophyll autofluorescence was excited at 405 nm and recorded above 630 nm. For counterstaining mitochondria, leaf tissue was incubated with 1 µM tetramethylrhodamine methyl ester (TMRM) for 30–60 min. TMRM was excited at 543 nm and recorded at 582–646 nm. For glutathione labelling in roots of Arabidopsis seedlings, intact seedlings were incubated with 100 µM monochlorobimane (MCB) and 50 µM propidium iodide (PI) for 30 min and imaged as reported earlier (Meyer *et al.*, 2001). For ratiometric imaging of  $E_{GSH}$  roGFP2-Grx1 was excited in multitrack mode with line switching between 488 nm illumination and 405 nm illumination. The roGFP2 fluorescence was collected with a 505–550 nm emission band-pass filter. Ratiometric image analysis was done as reported previously (Schwarzländer *et al.*, 2008) using a custom MATLAB program (Fricker, 2016).

## Results

### *gr2* T-DNA insertion allele causes early embryonic lethality

To investigate the role of GR2 for glutathione redox homeostasis, T-DNA insertion lines for *GR2* were identified and characterised. The T-DNA insertion lines *emb2360-1*, *emb2360-2*, *emb2360-3* (Tzafirir *et al.*, 2004), and *gr2-1* (SALK\_040170) were obtained from NASC. The T-DNA insertion in *gr2-1* was localised in the 8<sup>th</sup> intron (Fig. 1a) and the insertion site was confirmed by sequencing using a T-DNA left border primer. A population of

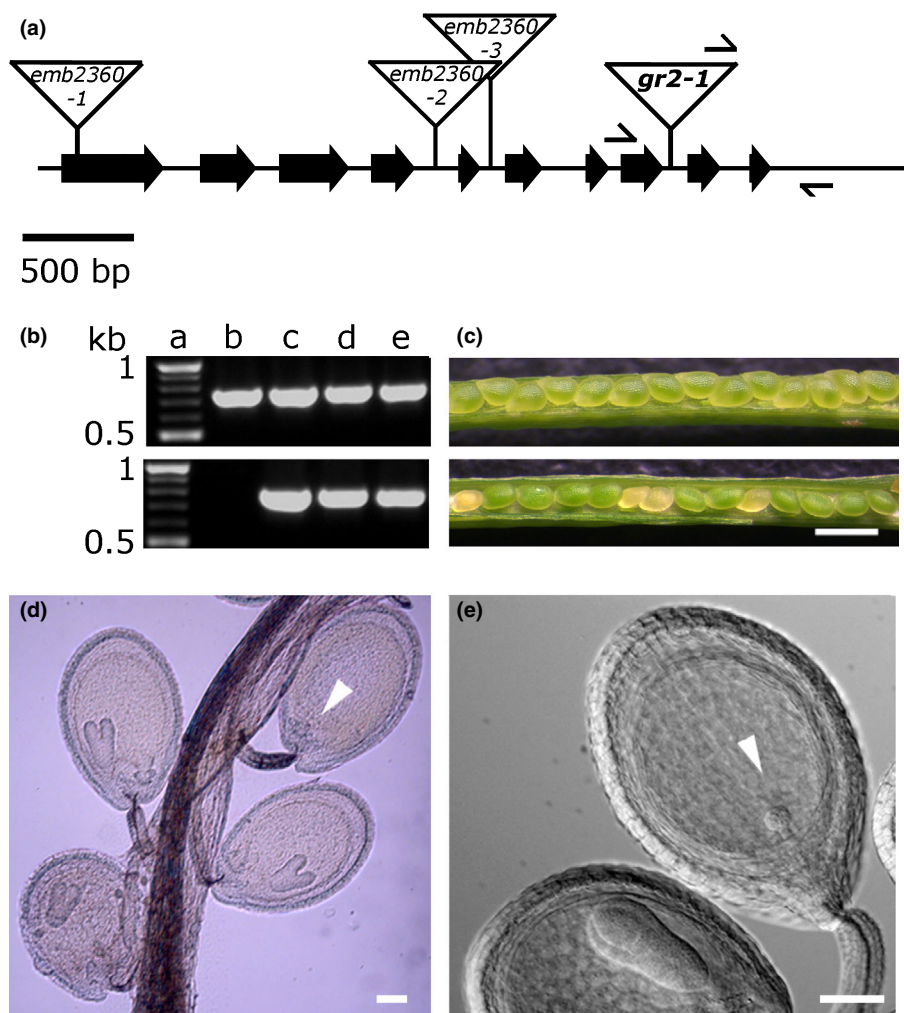


**Fig. 1** Isolation and phenotypic characterisation of Arabidopsis *gr2* null mutants. (a) Exon/intron structure of the Arabidopsis *GR2* gene (At3g54660). Exons are represented by large arrows and the triangles show the T-DNA insertions for three *emb2360* alleles ([http://seedgenes.org/SeedGeneProfile\\_geneSymbol\\_EMB\\_2360.html](http://seedgenes.org/SeedGeneProfile_geneSymbol_EMB_2360.html)) and the allele *gr2-1*. Primer binding sites for genotyping of *gr2-1* are indicated by black arrows. (b) Genotype analysis of different *gr2-1* lines. Upper panel: PCR performed with *GR2* gene-specific primers. Lower panel: PCR with a gene-specific primer and a primer for the left T-DNA border. Lane a: DNA marker: size is indicated in kb; Lane b: wild-type (WT); Lanes c–e: heterozygous *gr2-1* mutants. (c) Embryo-lethal phenotype associated with *gr2-1*. Immature siliques from self-fertilised WT (upper panel) and heterozygous *gr2-1* mutants (lower panel) were opened to observe segregation of seed phenotypes. Bar, 500 μm. 25% of the seeds in the *gr2* siliques show a lethal phenotype visible as white seeds. (d, e) Developing seeds of heterozygous *gr2-1* mutants were cleared using Hoyer's solution and analysed by bright field microscopy (d) and DIC microscopy (e). Arrowheads indicate white ovules containing embryos arrested at globular stage. Bars, 50 μm.

133 plants derived from a heterozygous *gr2-1* plant segregated with 85 kanamycin-resistant ( $\text{Kan}^{\text{R}}$ ):48 kanamycin-sensitive plants. This segregation of the antibiotic resistance in a 2 : 1 ratio ( $\chi^2 = 0.45$ ,  $P = 0.79$ ) indicates that homozygous *gr2-1* segregates as a single locus and is sporophytic lethal. Genotyping of soil-grown  $\text{Kan}^{\text{R}}$  plants confirmed that all  $\text{Kan}^{\text{R}}$  plants were heterozygous *gr2-1*, demonstrating that  $\text{Kan}^{\text{R}}$  is caused by the T-DNA in the *GR2* locus. Microscopic examination of immature siliques of heterozygous *gr2-1* mutants showed that 25% (31 : 97,  $\chi^2 = 0.04$  for a 1 : 3 segregation,  $P = 0.98$ ) seeds were white with embryos arrested at globular stage of development (Fig. 1d,e). Consistent segregation patterns and phenotypes were found for the three *emb2360* alleles ([http://seedgenes.org/SeedGeneProfile\\_geneSymbol\\_EMB\\_2360.html](http://seedgenes.org/SeedGeneProfile_geneSymbol_EMB_2360.html)), providing independent evidence for a link between *GR2* function and embryonic lethality. All further experiments were carried out with *gr2-1*, which is from now referred to as *gr2*.

### GR2 solely targeted to plastids rescues the lethal *gr2* phenotype

With the precedence of contradicting results regarding the sub-cellular localisation of *GR2* (Chew *et al.*, 2003; Yu *et al.*, 2013)

we attempted an orthogonal method to explore localisation and raised polyclonal antibodies against *GR2* (Fig. S2b). Immunogold labelling of *GR2* in leaf tissue of wild-type plants independently demonstrates its dual localisation (Fig. 2a,d). The early embryonic lethal phenotype of *gr2* may therefore be caused by mitochondrial or plastidic defects, or both. To resolve this, *gr2* mutants were complemented with organelle-specific *GR2* constructs. The endogenous signal peptide of 77 aa was replaced by the signal peptides SHMT<sub>TP</sub> for mitochondria or TK<sub>TP</sub> for plastids (Schwarzländer *et al.*, 2008; Albrecht *et al.*, 2014) (Fig. S1).

Compartment-specific complementation of *gr2* was initially done with *GR2* constructs driven by the *CaMV 35S* promoter (*35S<sub>pro</sub>*) (Fig. S1). T2 transformants (named *pc* for plastid complementation) were selected with Basta<sup>®</sup> and genotyped for the *gr2* locus to screen for successful complementation of the lethal phenotype. Transformation with *35S<sub>pro</sub>:TK<sub>TP</sub>-Δ<sub>1-77</sub>-GR2* resulted in 22 % of the progeny being homozygous for *gr2* consistent with the theoretical value of 25% rescued homozygous mutants (Table S2). From these complemented mutants three independent lines, named *pc-1*, *pc-2* and *pc-3*, were selected and characterised in more detail (Fig. S2). Protein gel blots of wild-type leaf extracts consistently revealed two distinct protein bands of *c.* 53 and *c.* 110 kDa (Fig. S2b). The 110 kDa protein band was less

intense than the 53 kDa band and most likely represents a GR2 homodimer. The unprocessed wild-type GR2 protein including the endogenous signal peptide of 77 aa has a predicted size of 61 kDa. The 53 kDa band detected in the protein gel blot likely corresponds to the mature processed protein with a predicted size of 52.7 kDa. This result indicates that cleavage of the endogenous GR2 signal peptide is the same for plastids and mitochondria. In *pc* lines overexpressing TK<sub>TP</sub>-GR2, a very strong increase in both bands was observed without significant change in the relative distribution between the two bands. Moreover, in all *35S<sub>pro</sub>:GR2* overexpression lines several additional protein bands with masses below that of GR2 may indicate partial degradation of GR2. Total GR activity in leaf tissue extracts was 49 nmol min<sup>-1</sup> mg<sup>-1</sup> for wild-type and *c.* 700 nmol min<sup>-1</sup> mg<sup>-1</sup> for the *pc* lines (Fig. S2c). This 15-fold increase is consistent with the pronounced increase in GR2 abundance observed in the *pc* lines. All *pc* lines showed wild-type-like GSH and GSSG levels with no changes in the GSH/GSSG ratio detectable by HPLC-based thiol analysis (Fig. S2d). At random time points in their development several T1 plants complemented with *35S<sub>pro</sub>:TK<sub>TP</sub>-Δ<sub>1-77</sub>GR2* unexpectedly showed wilted, dwarfed and purple coloured phenotypes, ultimately resulting in plant death before seed setting (Fig. S2a). This phenotype occurred irrespective of whether the genetic background of the respective plants was wild-type, *gr2*<sup>+/-</sup> or *gr2*<sup>-/-</sup>. Although not tested experimentally, the occurrence of plant death in wild-type and *gr2*<sup>+/-</sup> plants strongly suggests that the phenotype was caused by co-suppression of the endogenous *GR2* gene together with the transgene.

To avoid potential artefacts resulting from extremely high levels of GR2 protein and also to minimise the risk of silencing, *gr2* mutants were complemented with *GR2* driven by its endogenous promoter (Fig. S1). In this case, however, only 10% of the progeny, named *epc*, were found to be homozygous for *gr2* (Table S2). The lower frequency of the complementation with *GR2* driven by the endogenous promoter is most likely due to the much lower activity of this promoter compared with the *35S<sub>pro</sub>*. In some cases, the activity of the used *GR2<sub>pro</sub>* may not be sufficient to achieve full complementation and therefore cause premature abortion of homozygous *gr2* embryos.

By contrast, none of the transgenic lines transformed with either *35S<sub>pro</sub>:SHMT<sub>TP</sub>-Δ<sub>1-77</sub>GR2* or *GR2<sub>pro</sub>:SHMT<sub>TP</sub>-Δ<sub>1-77</sub>GR2* for mitochondrial targeting of GR2 was found to be a homozygous knockout for *gr2* (Table S2). Therefore, only *TK<sub>TP</sub>-Δ<sub>1-77</sub>GR2* constructs controlled by either the endogenous *GR2<sub>pro</sub>* or *35S<sub>pro</sub>* rescued the lethal *gr2* mutant, indicating that only plastid-localised GR2, but not the mitochondria-localised GR2, is essential for development. Correct targeting of both GR2 plastid complementation constructs was confirmed by immunogold labelling (Fig. 2b–d).

Three independent homozygous *gr2* mutants complemented with *GR2<sub>pro</sub>:TK<sub>TP</sub>-Δ<sub>1-77</sub>GR2* constructs were isolated and named *epc-1*, *epc-2* and *epc-3*, respectively. When grown on soil under short-day conditions, all three *epc* lines showed wild-type-like phenotypes in growth and development (Fig. 3a). GR2 protein levels in T1 plants with different genotypes with respect to the *gr2* locus were determined by protein gel blot analysis (Fig. 3b).

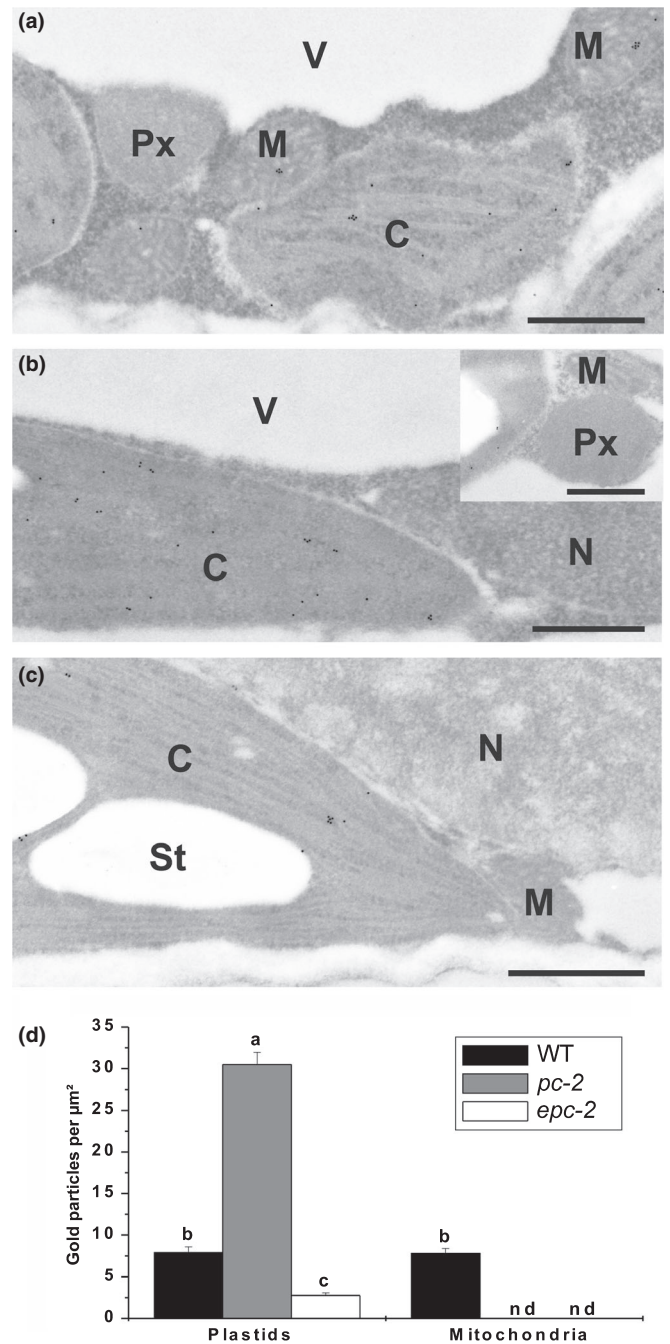


**Fig. 2** Immunogold localisation of GR2 in plastid-complemented Arabidopsis *gr2* deletion lines. Fixed and dissected mature leaves were probed with a primary antibody raised against Arabidopsis GR2. C, chloroplast; M, mitochondrion; Px, peroxisome; V, vacuole; N, nucleus; St, starch grain. Bars, 1 μm. (a) Wild-type (WT). (b) Line *pc-2* ('plastid-complemented') with TK<sub>TP</sub>-Δ<sub>1-77</sub>GR2 expressed from the *35S* promoter. (c) Line *epc-2* with TK<sub>TP</sub>-Δ<sub>1-77</sub>GR2 expressed from the endogenous GR2 promoter. (d) Quantitative analysis of gold particles observed in electron microscopy micrographs. Values are means ± SE and document the amount of gold particles per μm<sup>2</sup> in the respective organelle. Data were analysed by the Kruskal–Wallis test, followed by post hoc comparison according to Conover. Different lowercase letters indicate significant differences (*P* < 0.05). *n* > 60. nd, not detected.

Similar to wild-type and the  $35S_{pro}$  complemented lines, protein gel blot analysis of total protein extracts consistently revealed two bands of  $c.110$  kDa and  $c.53$  kDa, respectively, with the 53 kDa band being much more intense. In addition to the 53 and 110 kDa bands, protein extracts of  $TK_{TP}\Delta_{1-77}GR2$  transformants showed a third band with a size of  $c.55$  kDa. The appearance of this band suggests that import processing of the  $TK_{TP}\Delta_{1-77}GR2$  protein differed from wild-type GR2. Indeed, ChloroP predicts  $TK_{TP}\Delta_{1-77}GR2$  processing to result in a mature protein with a mass of 54.2 kDa. In all three homozygous  $gr2$  complementation lines only the 55 kDa protein was identified while the 53 kDa band was absent, further confirming at biochemical level that all three selected  $epc$  lines were indeed  $gr2$  null mutants successfully complemented with  $TK_{TP}\Delta_{1-77}GR2$ . Furthermore, the absence of a larger band of 61 kDa indicates that plastid import of GR2 was highly efficient without detectable traces of nonprocessed cytosolic protein. Protein gel blot analysis of plants transformed with  $GR2_{pro}:SHMT_{TP}\Delta_{1-77}GR2$  showed the same two-band pattern found in wild-type (Fig. 3b, lane d). Lack of additional bands suggests that the processed wild-type GR2 and processed  $SHMT_{TP}\Delta_{1-77}GR2$  proteins have similar

sizes, which is also supported by bioinformatics prediction by SIGNALP 3.0.

### Minute amounts of functional GR2 are sufficient for growth

GR activity of total protein extracts of the  $epc$  lines was  $60\text{ nmol min}^{-1}\text{ mg}^{-1}$  and therefore  $c.30\%$  lower than wild-type GR activity of  $90\text{ nmol min}^{-1}\text{ mg}^{-1}$  (Fig. 3c). Both, protein gel blot analysis and GR activity measurements of all three independent  $epc$  lines, showed that the amount of GR2 protein was significantly lower than in wild-type. This indicates that either promoter and/or enhancer elements other than the 2.1 kb fragment used here, may contribute to control the GR2 expression in wild-type plants, or that positional effects may have led to partial repression of GR2 in  $epc$  lines. The content of GSH and GSSG was comparable with wild-type plants (Fig. 3d).

The GR activity in  $epc$  lines is due to the  $GR2$  transgene and the endogenous GR1 activity, which had been reported to account for 40–60% of the total GR activity in leaves (Marty *et al.*, 2009; Mhamdi *et al.*, 2010). To further separate these activities and to

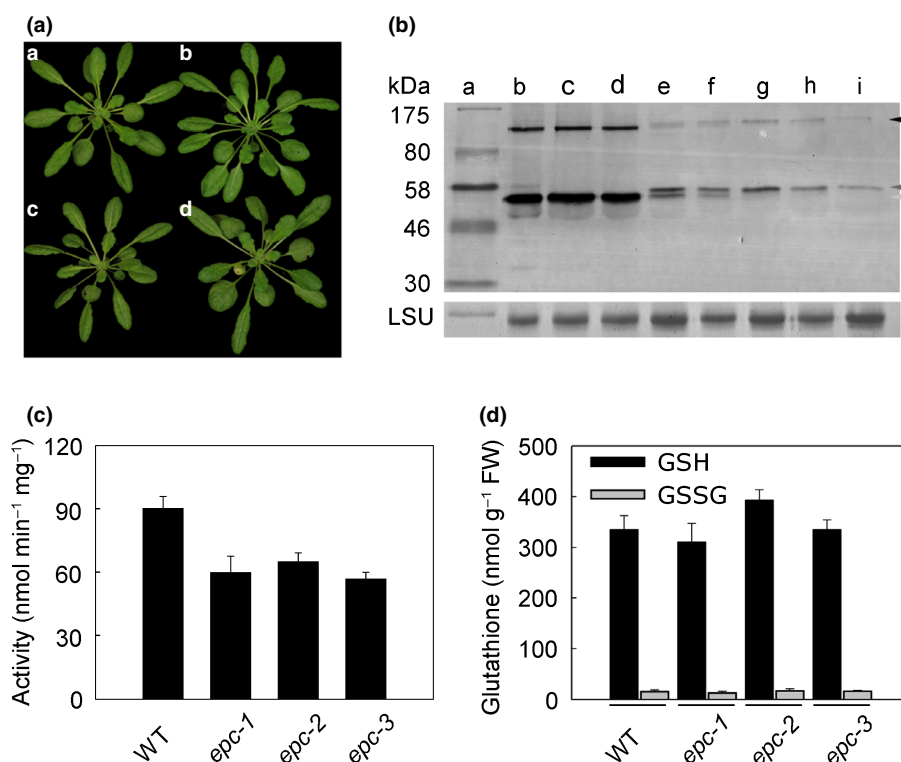


**Fig. 3** Characterization of Arabidopsis lines expressing plastid-targeted GR2 controlled by its endogenous promoter. (a) Growth phenotypes of wild-type (WT) 'a' and three independent homozygous  $gr2$  deletion mutants complemented with  $GR2_{pro}:TK_{TP}\Delta_{1-77}GR2$ :  $epc-1$  'b',  $epc-2$  'c',  $epc-3$  'd'. All transgenic plants were from the Basta<sup>®</sup>-selected T1 generation. (b) Protein gel blot analysis of transgenic Basta<sup>®</sup>-selected T1 lines transformed with complementation constructs driven by the endogenous  $GR2$  promoter and targeted to either mitochondria or plastids. Loading was as follows: a: Prestained molecular mass standard, b: WT, c: WT transformed with  $GR2_{pro}:SHMT_{TP}\Delta_{1-77}GR2$ , d:  $gr2^{+/-}$  transformed with  $SHMT_{TP}\Delta_{1-77}GR2$ , e: WT transformed with  $GR2_{pro}:TK_{TP}\Delta_{1-77}GR2$ , f:  $gr2^{+/-}$  transformed with  $GR2_{pro}:TK_{TP}\Delta_{1-77}GR2$ , g–i: three independent homozygous  $gr2$  deletion lines transformed with  $GR2_{pro}:TK_{TP}\Delta_{1-77}GR2$  ( $epc-1$ ,  $epc-2$  and  $epc-3$ ). Arrowheads indicate protein bands with the size of 110 kDa (black), 55 kDa (dark grey) and 53 kDa (light grey). The blot was probed with anti-GR2. (c) GR activity in total protein extract from leaves. Proteins were extracted from WT and T2 plants of the homozygous  $gr2$  lines  $epc-1$ ,  $epc-2$  and  $epc-3$ . Means  $\pm$  SD of three independent plants of each line are shown. (d) Contents of oxidised and reduced glutathione. After extraction of leaf tissue of 5-wk-old plants reduced glutathione (GSH) and glutathione disulfide (GSSG) were determined by high performance liquid chromatography (HPLC). Means  $\pm$  SD of six independent plants of each line are shown.

better assess the requirement for GR2 necessary for normal growth, we generated a double heterozygous *gr1<sup>+/-</sup> gr2<sup>+/-</sup>* plant and complemented this with the same *GR2<sub>pro</sub>:TK<sub>TP</sub>-Δ<sub>1-77</sub>GR2* construct used before. From the F2 progeny we selected two homozygous *gr1 gr2* double knockouts that expressed GR2 exclusively in the plastids (lines *epc-9* and *epc-27*). These *gr1 gr2* plants did not show any obvious phenotype in their growth and development during the vegetative phase under standard growth conditions (Fig. 4a). The total GR activity in leaf extracts was only between  $10 \pm 2.6$  and  $1.5 \pm 0.1$  nmol mg<sup>-1</sup> min<sup>-1</sup> compared with  $53.2 \pm 3.5$  nmol mg<sup>-1</sup> min<sup>-1</sup> in wild-type leaves (Fig. 4b). For comparison, *gr1* mutants and the plastid-complemented *gr2* mutant (*epc-2*) showed intermediate GR-activities of  $37.5 \pm 2.6$  and  $24.2 \pm 2.6$  nmol mg<sup>-1</sup> min<sup>-1</sup>, respectively (Fig. 4b). Lack of GR1 in *gr1-1* and in *gr1 gr2* double deletion mutants consistently resulted in an increase in total glutathione (Fig. 4c). Further analysis of the glutathione pool revealed that this increase was largely due to an increase in GSSG, which was *c.* six-fold higher compared with wild-type controls (Fig. 4d). If at all, plastid-specific complementation of *gr2* resulted in only a minor increase in glutathione (Figs 3d, 4c).

To further test for mitochondrial GR activity, we first isolated mitochondria from the plastid-complemented line *epc-2* and determined the specific GR activity in mitochondrial extracts. While mitochondria isolated from wild-type plants had a specific GR activity of 47.9 nmol min<sup>-1</sup> mg<sup>-1</sup>, mitochondria from *epc-2* contained an activity of 2.4 nmol min<sup>-1</sup> mg<sup>-1</sup> (Fig. 5a). Identity of mitochondrial preparations was confirmed by detection of the mitochondrial marker peroxiredoxin II F (PRXII F; (Finkemeier

*et al.*, 2005)). Further analysis of the respective extracts indicated that GR2 was absent in *epc-2* mitochondria (Fig. 5c). Hybridisation of the respective protein blots with a GR1 antibody (Marty *et al.*, 2009) revealed that the mitochondrial fraction also contained GR1 (Fig. 5c) which can be accounted for by the presence of peroxisomes that contain GR1, in mitochondrial preparations from Arabidopsis seedlings (Sweetlove *et al.*, 2007). No GR activity was found in mitochondria isolated from line *epc-27* (Fig. 5b). Protein gel blots confirmed absence of both GR1 and GR2 from *epc-27* mitochondria (Fig. 5d).

### Glutathione deficiency partially suppresses embryo lethality of *gr2*

Early embryonic lethality of *gr2* null mutants may be explained by lack of appropriate backup systems for GSSG reduction, or an additional, yet unknown, moonlighting function (Jeffery, 2009) of plastidic GR2. By law of parsimony we elucidated whether the early embryonic lethal phenotype is caused solely by accumulation of GSSG in plastids. For this, we reasoned that GSH-deficiency would necessarily go along with deficiency of GSSG and therefore might suppress the early embryonic lethal phenotype of *gr2*. To test this hypothesis, *gr2* was crossed with the two GSH-deficient mutants *rml1* and *gsh1-1*, which are both compromised in the first step of GSH biosynthesis catalysed by glutamate-cysteine ligase (GSH1) and contain strongly decreased glutathione levels (Vernoux *et al.*, 2000; Cairns *et al.*, 2006). While *rml1* completes embryogenesis and germinates, the null mutant *gsh1-1* reaches U-turn stage before it dies (Vernoux *et al.*, 2000; Cairns

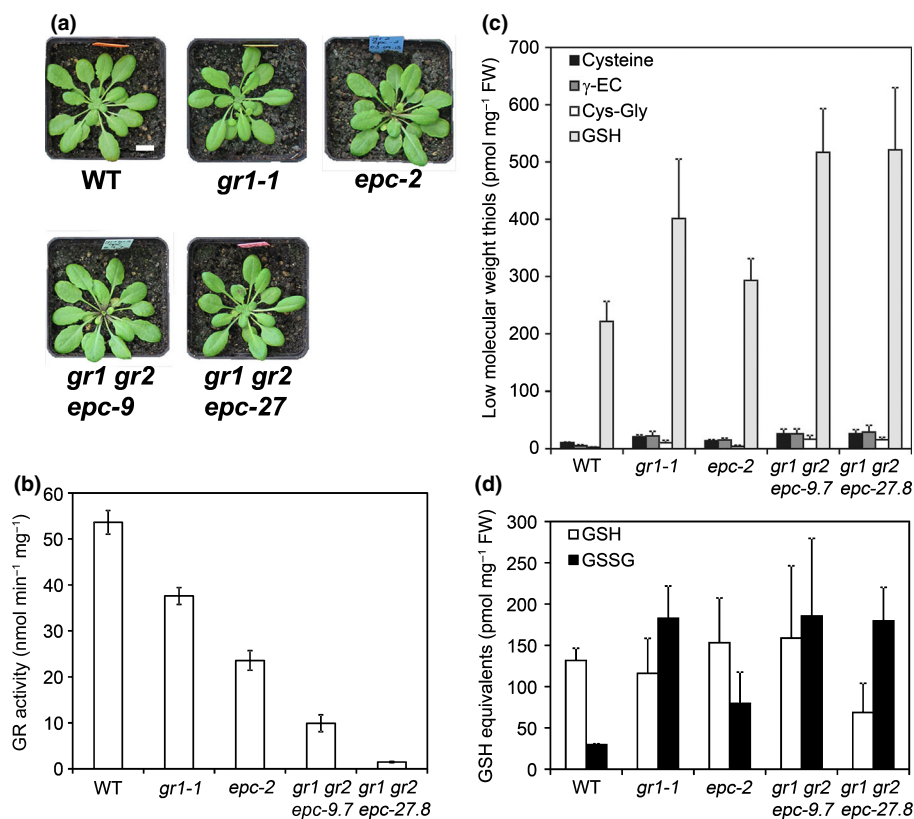


**Fig. 4** Glutathione reductase activity and low-molecular-weight thiols of Arabidopsis *gr1 gr2* double homozygous mutants complemented with plastid-targeted GR2. (a) Rosette phenotypes of plants grown on soil for 6 wk under short-day conditions (8 h : 16 h, light : dark). Bar, 1 cm. (b) GR activity in total protein extracts from leaves. Proteins were extracted from wild-type (WT), *gr1*, plastid-complemented *gr2* (*epc-2*) and two *gr1 gr2* double mutants (*epc-9* and *epc-27*) that were complemented with *GR2<sub>pro</sub>:TK<sub>TP</sub>-Δ<sub>1-77</sub>GR2*. Means  $\pm$  SD of three independent plants of each complemented line are shown. (c) Low-molecular-weight thiols analysed by HPLC from leaf extracts. GSH in this case refers to total glutathione. Means  $\pm$  SD, *n* = 3. (d) Reduced glutathione (GSH) and glutathione disulfide (GSSG) determined by HPLC in leaf extracts. Means  $\pm$  SD, *n* = 3.

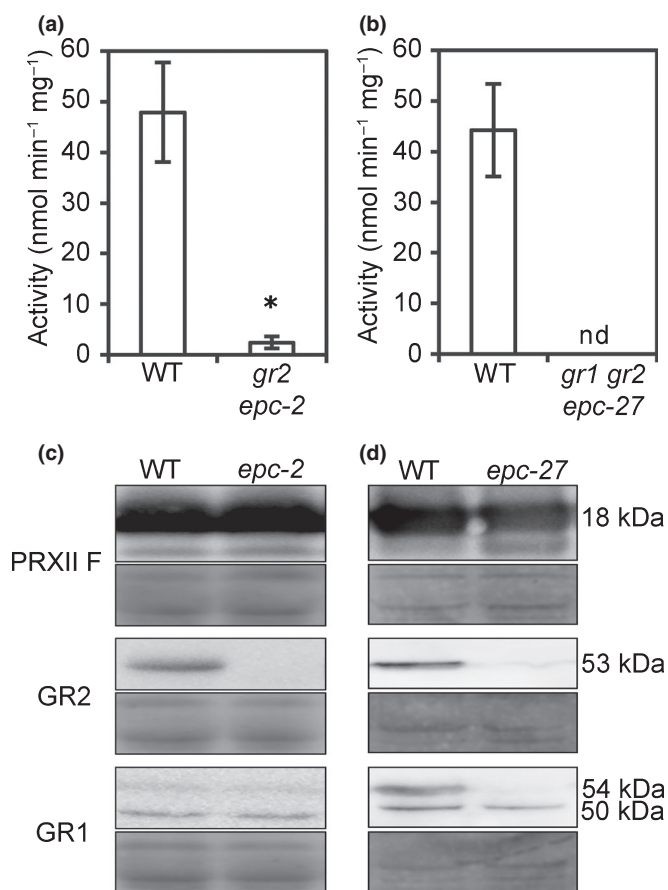


**Fig. 5** Glutathione reductase activity in isolated mitochondria. Intact mitochondria were isolated from 2-wk-old hydroponically grown *Arabidopsis* plants (wild-type (WT) and *epc-2* lacking endogenous GR2, or *epc-27* lacking both endogenous GRs, respectively). Activities represent the means from four independent preparations with six technical replicates. Error bars represent SD. (a, b) GR activity. nd, not detected; \* indicates  $P < 5 \times 10^{-4}$ . (c, d) Protein gel blots of PRXII F, GR2 and GR1 in mitochondrial preparations. Loading controls were stained with amido black. In addition to GR1 (54 kDa), the GR1 antibody detected also a smaller protein of *c.* 50 kDa (Fig. 5d). This band, however, appears to result from a side activity against another mitochondrial protein that is detectable in concentrated isolated mitochondria, but not in whole leaf extracts (Fig. S3b). Mitochondria contain two lipoamide dehydrogenases (MTLPD1 and MTLPD2) that are closely related to GR and are both predicted with a molecular mass of 49.9 kDa after cleavage of the mitochondrial target peptide (Lutziger & Oliver, 2001). Therefore it is likely that the additional band results from a crossreaction of the antibody with MTLPDs.

*et al.*, 2006). While no double homozygous *rml1 gr2* could be found (Fig. S4) the *gr2 gsh1* cross and selfing of a double heterozygous plant resulted in *c.* 24 % aborted seeds albeit with a distinct phenotypic variation (Fig. 6c). Closer inspection of the aborted seeds revealed that *c.* 1/4 of seeds were aborted later than the typical *gr2* embryo, which were seen as white turgescence ovules (Fig. 6c). Indeed developing seeds collected from a selfed double heterozygous *gr2<sup>+/-</sup> gsh1<sup>+/-</sup>* plant showed a segregation of their embryos in 334 U-turn:92 globular:30 torpedo (12:3:1,  $\chi^2 = 0.76$ ,  $P = 0.34$ ) (Fig. 6d–g). This result indicates that GSH-deficiency caused by *gsh1* partially suppressed the early

embryo-lethal *gr2* phenotype extending development until the torpedo stage. Although it cannot be fully excluded that the combination of severe mutants may lead to some unknown pleiotropic effects, we interpret the observed suppression as an indication for GSSG toxicity as the cause of the early embryo lethality in the absence of GR2 from the plastid stroma.

#### The mitochondrial glutathione pool of plastid-complemented *gr2* mutants shows increased oxidation

Full viability of plastid-complemented *gr2* plants suggests that mitochondria can maintain their function in the absence of GR2. This suggests that they are either able to cope with a fully oxidised glutathione pool made up of GSSG, or other mechanisms of maintaining reduction exist. Candidate mechanisms include GSSG export from the matrix for reduction in the cytosol as well as an alternative enzymatic system for efficient internal GSSG reduction. To address this question, we tested whether  $E_{\text{GSH}}$  in the mitochondrial matrix of mutants lacking GR2 in mitochondria is more oxidised than in wild-type controls. Plastid-complemented *gr2<sup>-/-</sup>* mutants (*epc-2*) were transformed with the  $E_{\text{GSH}}$  biosensor roGFP2-Grx1 targeted to the mitochondrial matrix (Albrecht *et al.*, 2014). roGFP2 constructs were expressed from *35S<sub>pro</sub>* and we deliberately selected strongly expressing lines in which part of the sensor proteins remained in the cytosol and the nucleus (Figs 7, S5). The resulting dual localisation of roGFP2-Grx1 allowed simultaneous ratiometric imaging of roGFP2 in both compartments by confocal microscopy. Because the roGFP2-Grx1 in the cytosol and the nucleus provides an internal control for close-to-complete sensor reduction (Meyer *et al.*, 2007; Schwarzländer *et al.*, 2008) the ratiometric images are informative without any further treatment with reducing and oxidising compounds. While the merge of the raw images collected after excitation at 405 nm and 488 nm in wild-type seedlings show similar green colour in cytosol and mitochondria (Fig. 7a) the same merge for the plastid-complemented *gr2<sup>-/-</sup>* mutant shows a pronounced difference: Cytosol and nucleus appear in green as in the wild-type control, while the mitochondria appear in yellow because the fluorescence in the 488 nm channel decreased and the fluorescence in the 405 nm channel increased (Fig. 7b). The differential behaviour of the signals in mitochondria and the cytosol is even more obvious after ratiometric analysis, which shows a partial oxidation of roGFP2-Grx1 in the GR2-deficient mitochondria. The degree of sensor oxidation can be estimated to approximately the midpoint of the sensor, that is *c.* 50%. This corresponds to a pronounced shift in mitochondrial matrix  $E_{\text{GSH}}$  of *c.* 30 mV, but is remains far from a complete oxidation of the matrix glutathione pool.

#### The mitochondrial ABC transporter ATM3 has a critical function in GR2-deficient mitochondria

Export of GSSG from the mitochondrial matrix and subsequent reduction by cytosolic GR1 activity would provide an alternative mechanism to adjust the matrix  $E_{\text{GSH}}$ . To elucidate whether the



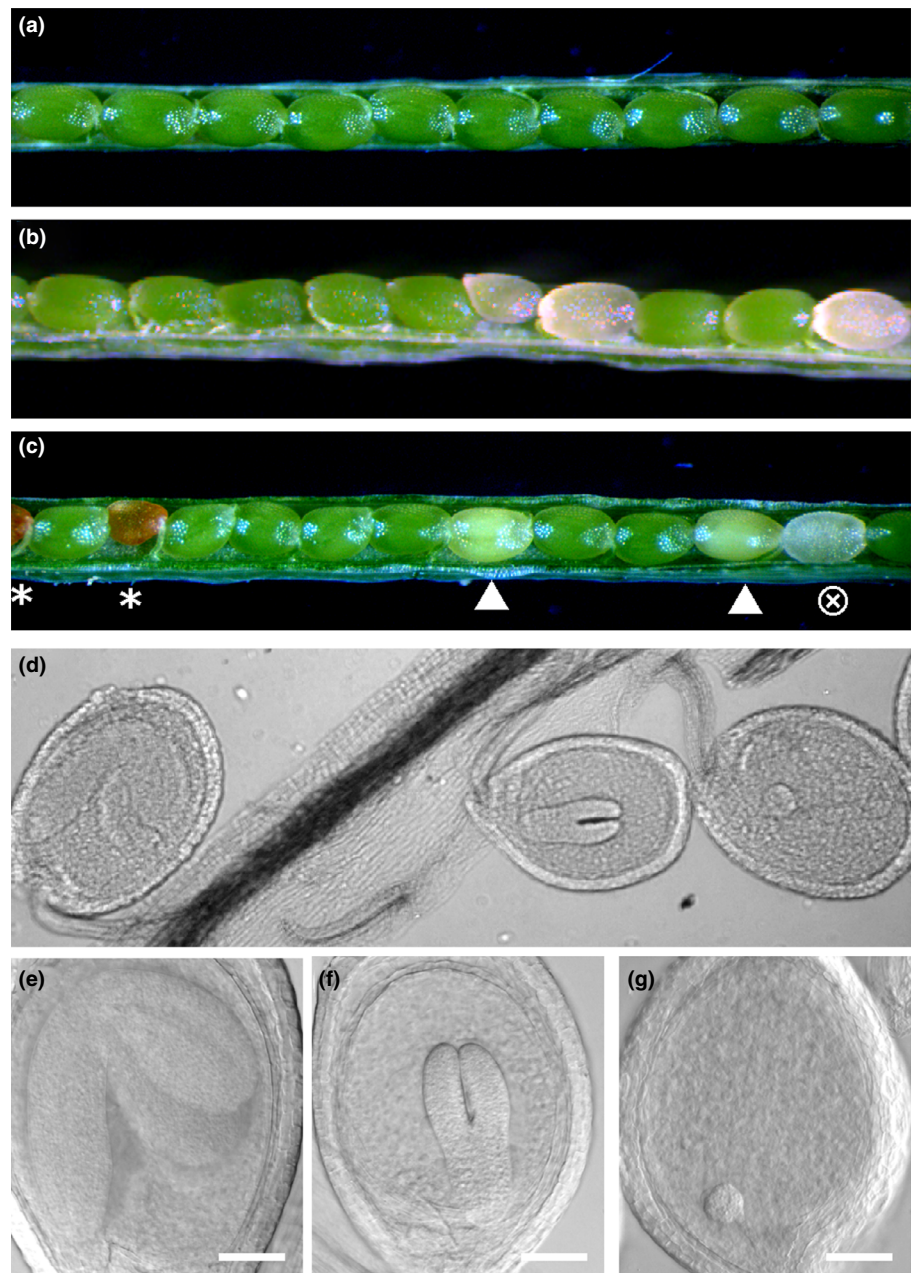


**Fig. 6** Characterization of *Arabidopsis gr2 gsh1* double mutants. (a) Wild-type (WT) silique at 14 d after fertilisation (DAF). (b) Silique of self-fertilised heterozygous *gr2* plant displaying 25% aborted seeds. (c) Silique of self-fertilised double heterozygous *gr2<sup>+/-</sup> gsh1<sup>+/-</sup>* plant displaying segregation of green WT seeds, partially bleached *gsh1* seeds (arrowhead), brownish early aborted *gr2* seeds (\*), and transparent seeds (X) that remain fully turgescient significantly longer than *gr2* seeds. (d–g) DIC images of ovules developed in a silique of a self-fertilised double heterozygous *gr2<sup>+/-</sup> gsh1<sup>+/-</sup>* plant 14 DAF. Bars, 50 µm.

GSSG export ability of *ATM3* could help to maintain low GSSG levels and support the mitochondrial GR2 activity, we crossed the mutant *gr2 epc2* deficient in mitochondrial GR2 with *atm3-4*, and isolated the double mutant. *atm3-4* is a relatively weak mutant allele, with low expression of functional *ATM3* due to a 39-nucleotide deletion in the promoter (Bernard *et al.*, 2009). The *atm3-4 gr2 epc2* double mutant showed an enhanced phenotype compared with both the *gr2 epc2* and *atm3-4* parents, with short roots at seedling stage and smaller rosettes when grown on soil (Fig. 8). Leaves appeared chlorotic and displayed a significantly lower  $F_v/F_m$  (Fig. 8d). These observations suggest synergistic action of the two mutations with lack of mitochondrial GR2 causing increased GSSG levels in the matrix that cannot be

efficiently decreased when *ATM3* protein levels are strongly depleted.

#### NADPH-dependent thioredoxin reductases backup mitochondrial GR2

Both, NTRA and NTRB, are known to be dual-targeted to the cytosol and mitochondria (Reichheld *et al.*, 2005). Based on the observation that the NTR/TRX system efficiently reduces GSSG in the cytosol (Marty *et al.*, 2009) we hypothesised that NTRA and NTRB together with mitochondrial TRXo1 and o2 (Yoshida & Hisabori, 2016), or TRXh2 (Meng *et al.*, 2010) may provide a functional backup system for mitochondrial GR2. To further

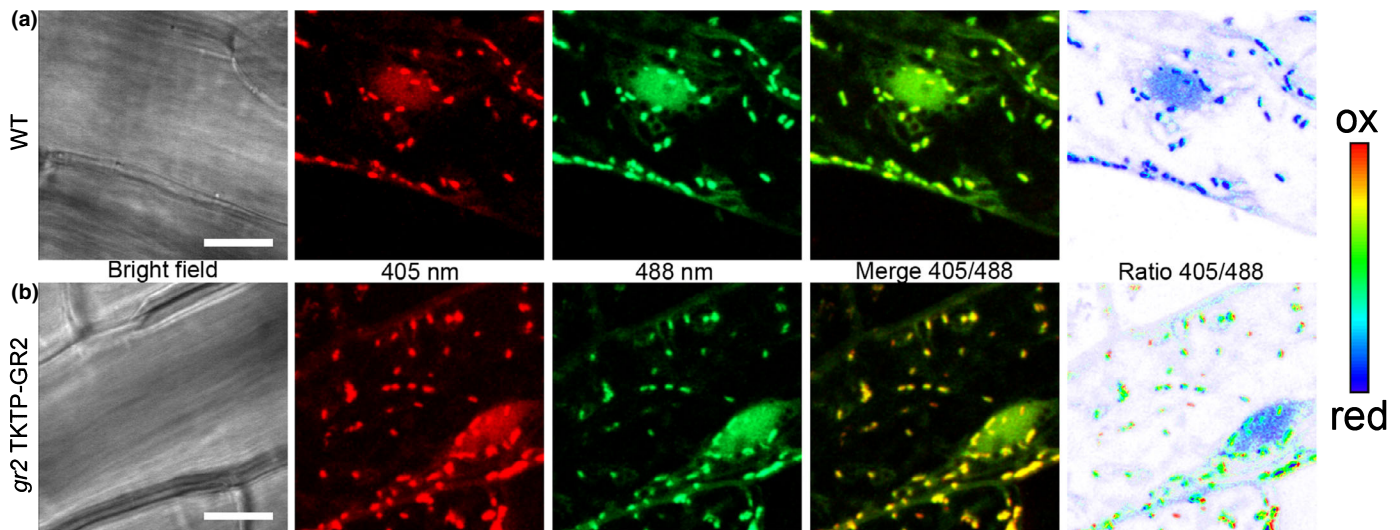


**Fig. 7** Simultaneous imaging of the local glutathione redox status in mitochondria and the cytosol of Arabidopsis seedlings. The ratiometric redox probe roGFP2-Grx1 was expressed with a SHMT<sub>TP</sub> mitochondrial targeting sequence driven by a *35S<sub>pro</sub>*. After transformation lines with residual roGFP2-Grx1 in the cytosol were selected and used for simultaneous redox imaging in mitochondria and the cytosol. Images show hypocotyl cells in wild-type (WT) seedlings (a) or plastid-complemented *gr2*<sup>-/-</sup> seedlings (b). Images taken after excitation at 405 nm are false colour coded in red and images taken after excitation at 488 nm are coded in green in order to visualise a pronounced colour change in the merge image from green to yellow in the mitochondria. Bars, 10 μm.

support this hypothesis, we also tested mitochondrial TRXs for their ability to reduce GSSG *in vitro* and determined steady-state kinetic parameters for GSSG for TRXh2, TRXo1 and GR2. In conjunction with NTRA recombinant TRXh2 and TRXo1 are both capable of reducing GSSG, albeit with  $K_m$  values of only  $2\text{--}4 \times 10^3 \mu\text{M}$ , which is nearly 100-fold higher than the  $K_m$  of GR2 (13 μM) (Fig. 9). While the efficiency  $k_{cat}/K_m$  of GR2 approximates the diffusion limit,  $k_{cat}/K_m$  for both TRXs is *c.* 1000-fold lower. The GSSG reduction activity of both TRXs is independent of which NTR isoform is available for TRX reduction (Fig. S6).

To further test the hypothesis that mitochondrial NTRs provide the rescue for lack of mitochondrial GR2, we generated a cross between an *ntra ntrb* double null mutant and a homozygous *gr2* complemented with plastid-targeted GR2 (Fig. S7). From this cross, F<sub>3</sub> plants expressing GR2 were preselected by Basta<sup>®</sup> to ensure only GR2 complemented plants to be maintained. Next, plants segregating for *ntrb* only were selected through genotyping, and selfed. 71 tested F<sub>4</sub> progeny segregated for the mutant allele *ntrb* 23 *NTRB/NTRB* : 48 *NTRB/ntrb* : 0 *ntrb/ntrb* ( $\chi^2 = 0.03$ ,  $P > 0.95$ ) indicating that homozygous *ntra ntrb gr2* triple mutants are not viable. The 1 : 2 segregation of viable plants suggested that the lethal effect of *ntra ntrb gr2* is not gametophytic but rather manifests itself only after fertilisation. Consistent with this, viability staining of pollen resulted in nearly 100 % viable pollen (Fig. S8). To further confirm full viability of *ntra ntrb gr2* pollen during pollen tube growth, we backcrossed the *ntra/ntra NTRB/ntrb gr2/gr2 plGR2* plant to wild-type. This cross resulted in a 1 : 1 segregation for *ntrb* ( $\chi^2 = 0.7$ ,  $P = 0.34$ ; Table S3a). Similarly, the reverse cross of wild-type pollen to an *ntra/ntra NTRB/ntrb gr2/gr2 plGR2* triple mutant resulted in a 1 : 1 segregation for *ntrb* ( $\chi^2 = 0.34$ ,  $P = 0.58$ ; Table S3b). These

results showed that both pollen and oocytes carrying all three mutant alleles are fully viable.

Developing siliques from self-fertilised *ntra/ntra NTRB/ntrb gr2/gr2 plGR2* plants by contrast contained many aborted seeds (Fig. 10a,b) supporting that the lethal phenotype was established at the diploid stage. However, the overall abortion rate of 13.4% in siliques collected from 10 randomly selected plants was significantly below the expected 25 % (114 aborted seeds out of 852 seeds;  $\chi^2 = 61.35$ ,  $P \ll 0.001$ ). A closer inspection of seedlings germinated from these seeds indicated some barely viable seedlings that ceased growth *c.* 3 wk after germination and died (Fig. 10c). PCR genotyping confirmed that these seedlings were homozygous for the segregating allele *ntrb* (Fig. 10d,e).

## Discussion

### GR2 is indispensable in plastids

Appropriate detoxification of H<sub>2</sub>O<sub>2</sub> produced during normal metabolism or in response to environmental stress is mandatory to ensure maintenance of sufficiently reducing conditions for normal metabolism (Moller *et al.*, 2007; Waszczak *et al.*, 2018). The glutathione-ascorbate cycle has attained much attention and connects H<sub>2</sub>O<sub>2</sub> detoxification via ascorbate peroxidases ultimately to the local glutathione pool with GSH providing the required electrons (Foyer & Noctor, 2011). The generated GSSG is subsequently reduced back to GSH by GRs with electrons provided by NADPH. While in Arabidopsis GR1 activity in the cytosol and peroxisomes can be substituted to a sufficient extent by the cytosolic NTS to avoid lethality of null mutants (Marty *et al.*, 2009), *gr2* null mutants are early embryonic lethal (Bryant *et al.*, 2011; Ding *et al.*, 2016b). Our results unanimously show

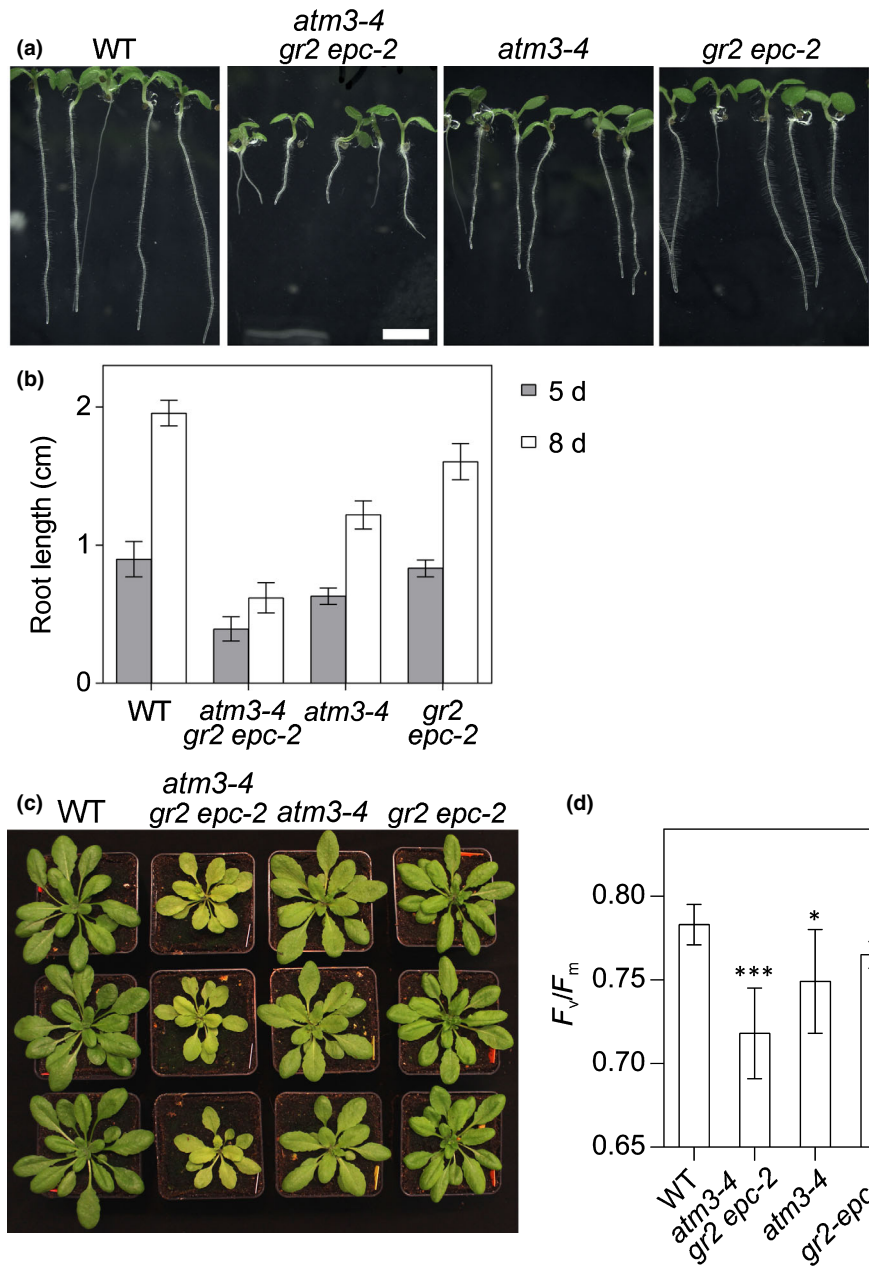


**Fig. 8** Arabidopsis *atm3-4 gr2 epc2* double mutants show a semidwarf and chlorotic phenotype. (a) Here, 8-d-old seedlings of the double mutant compared with wild-type (WT) and single mutants are shown. Bar, 0.5 cm. (b) Root length of the mutants compared with WT. Plants were grown on half-strength Murashige and Skoog ( $\frac{1}{2}$ MS) medium containing 0.5% sucrose and 0.8% phytagel for 5–8 d under long-day conditions after stratification for 2 d (means  $\pm$  SD,  $n = 5$ –12). (c) Plants were grown under long-day conditions for 4 wk. (d) Chlorophyll fluorescence of 4-wk-old plants grown on soil under long-day conditions (means  $\pm$  SD,  $n = 7$ ). The statistical analysis (one-way ANOVA with post hoc Holm–Sidak comparisons for WT vs mutant) indicates significant changes; \*,  $P \leq 0.05$ ; \*\*\*,  $P \leq 0.001$ .

that GR2 is dual-targeted to plastids and mitochondria but is essential only in plastids.

In the absence of sufficient amounts of GR2 in plastids continued detoxification even of low amounts of  $H_2O_2$  inevitably leads to a gradual increase in GSSG (Fig. 4) consistent with earlier observations on Arabidopsis plants with diminished GR2 activity (Yu *et al.*, 2013; Ding *et al.*, 2016b). While an increased GSSG concentration necessarily leads to a shift of  $E_{GSH}$  towards less negative values, a similar shift can also be caused by depletion of GSH (Meyer *et al.*, 2007; Aller *et al.*, 2013). The GSH-deficient mutant *gsb1* completes embryogenesis up to the seed maturation phase because maternal tissues provide a minimum amount of GSH to the embryo (Cairns *et al.*, 2006; Lim *et al.*, 2014). In *rml1*, the very low GSH content results in an  $E_{GSH}$  of *c.*  $-260$  mV (Aller *et al.*, 2013). Despite the pronounced shift in

$E_{GSH}$  the situation is not deleterious *per se*. Partial suppression of the early embryo arrest in *gr2 gsb1* double mutants rather points at the accumulation of GSSG being toxic. The severely restricted ability to build up normal GSH levels initially helps keeping the GSSG concentration low and enables embryos to develop beyond globular stage. However, the arrest at torpedo stage still occurs much earlier than the arrest in *gsb1* during seed maturation. This strongly suggests that, even without normal levels of GSH, GSSG quickly accumulates to toxic levels in plastids if no GR2 is present. Plastids apparently have no backup system for GSSG reduction and no (or insufficient) ability to export GSSG to the cytosol for reduction. In developing Arabidopsis embryos, the first chloroplasts start differentiating and greening with the initiation of cotyledons at heart stage (Mansfield & Briarty, 1991). This suggests that the accumulation of GSSG in globular

embryos is light-independent. Silencing of GR2 in mature plants indicates that light-dependent reduction of GSSG via plastidic TRXs may not be sufficient to maintain normal growth. This suggests that, in contrast to the cytosolic NTS, the plastidic FTR/TRX system cannot fully compensate for the lack of GR activity. This conclusion is consistent with observations that Arabidopsis mutants with RNAi-based depletion of GR2 develop early senescence (Ding *et al.*, 2016b), and with current findings in *Physcomitrella patens* plants lacking organellar GR, where stromal  $E_{\text{GSH}}$  is oxidised but not rescued by active photosynthetic electron transport (Müller-Schüssele *et al.*, 2019). Developmental arrest of *gr2* mutants at globular stage before chloroplast differentiation indicates that the accumulation of GSSG is not related to photosynthesis as a possible source of ROS (Foyer & Noctor, 2009), but rather to other basic metabolic processes. Possible processes include the formation of GSSG through reduction of oxidised GRX by GSH (Begas *et al.*, 2017) and the reduction of adenosine 5'-phosphosulfate by GSH (Bick *et al.*, 1998). In addition, several metabolic pathways in plastids involve oxidation steps in which molecular oxygen is reduced to  $\text{H}_2\text{O}_2$ . The reactions include the pyridoxal 5'-phosphate salvage pathway in which the plastidic pyridoxine/pyridoxamine 5'-phosphate oxidase produces one molecule  $\text{H}_2\text{O}_2$  (Sang *et al.*, 2011), the oxidation of L-aspartate by L-aspartate oxidase in the early steps of NAD biosynthesis (Katoh *et al.*, 2006), and the three-step oxidation of protoporphyrinogen IX to protoporphyrin IX by the enzyme protoporphyrinogen oxidase PPOX (Koch *et al.*, 2004; Mochizuki *et al.*, 2010). Nothing is known about the absolute amounts of  $\text{H}_2\text{O}_2$  produced along these pathways but it needs to be emphasised that a submicromolar increase in GSSG would generate already a massive oxidative shift in  $E_{\text{GSH}}$  (Meyer *et al.*, 2007), which is presumed to result in toxic effects.

Minute amounts of GR2 activity are necessary to avoid accumulation of GSSG to toxic levels. GR, in general, has been reported to be highly active with a very low  $K_m$  for GSSG leaving only low nanomolar traces of GSSG (Veech *et al.*, 1969). This activity dominates  $E_{\text{GSH}}$  *in vivo* keeping it highly reduced as confirmed by *in vivo* imaging with roGFP-based probes (Marty *et al.*, 2009; Schwarzländer *et al.*, 2016). Accumulating GSSG may interfere with fundamental plastidic processes, such as transcription, translation and enzymatic functions. For instance, fatty acid biosynthesis is vital in developing oilseed embryos and involves the redox-regulated heteromeric plastidic acetyl-CoA-carboxylase (ACCase) (Ke *et al.*, 2000; Sasaki & Nagano, 2004; Bryant *et al.*, 2011). The extraordinary importance of plastidic ACCase for embryo development is further supported by the early embryo-lethal phenotype of null mutants for BCCP1 (Li *et al.*, 2011). One of four ACCase subunits, CT $\beta$  (AtCg00500, AccD), is plastid encoded. Therefore, interfering with thiol switches regulating the plastidic gene expression machinery (Dietz & Pfannschmidt, 2011) or vital enzyme activities would constitute one possible scenario to account for our observations. Another possible toxic effect of GSSG is the disruption of Fe-S cluster transfer by monothiol GRXs which involves binding of GSH as a cofactor on its backbone (Moseler *et al.*, 2015). If present in sufficiently high

concentrations GSSG may interfere with GSH binding and disrupt Fe-S coordination (Berndt *et al.*, 2007). Plastids contain two monothiol GRXs of which GRXS16 carries an additional regulatory disulfide that is responsive to GSSG (Zannini *et al.*, 2019). GSSG-mediated oxidation of GRXS16 modulates its oxidoreductase function and enables protein glutathionylation or other oxidative modification of protein thiols. While analysis of the thiol proteome is not possible in globular embryos at this stage, massive global changes in the oxidation of the protein thiols were found in the proteome of *gr2* mitochondria (Nietzel *et al.*, 2019). Dissecting the mechanistic cause of embryo lethality is beyond the scope of this work, but promises intriguing novel insights into the role of redox dynamics in organelle biogenesis and early plant development.

### ATM3 and the mitochondrial TRX system safeguard the matrix $E_{\text{GSH}}$

Direct comparison of cytosol and mitochondrial matrix in plastid-complemented *gr2* mutants clearly showed that the readout of roGFP2-Grx1 was shifted to higher ratio values indicating a shift in the local  $E_{\text{GSH}}$  towards less negative values. While roGFP2 in the cytosol of plastid-complemented *gr2* lines is almost fully reduced indicating an  $E_{\text{GSH}}$  of  $-310$  mV or even more negative, roGFP2 in the mitochondrial matrix is clearly partially oxidised. The observed degree of sensor oxidation of *c.* 50 % would indicate an  $E_{\text{GSH}}$  of  $-280$  mV assuming a matrix pH of 7.0 ( $-310$  mV at pH 7.5). In a solution with estimated 2 mM GSH this point would be reached with *c.* 200 nM GSSG. This calculation shows that the amount of GSSG determined by HPLC in plants extracts is a significant overestimation of the amount of GSSG really present in the respective subcellular compartment. This is in line with earlier conclusions on sensor-based subcellular  $E_{\text{GSH}}$  measurements (Meyer & Dick, 2010; Schwarzländer *et al.*, 2016).

Although we showed that GSSG accumulation in plastids is causing embryo lethality, plants lacking GR2 in mitochondria have no obvious phenotype under control conditions. This is consistent with observations that found GR2 primarily responsible for maintaining photosynthetic processes (Ding *et al.*, 2016a). Two possible scenarios can be drawn to explain this observation: (1) GSSG can be exported to the cytosol to get reduced by GR1, or (2) GSSG is reduced in the matrix by other enzymes. Knock-down mutants with a severely limited ATM3 capacity have been shown earlier to have a less negative  $E_{\text{GSH}}$  in the mitochondrial matrix than wild-type (Schaedler *et al.*, 2014). The pronounced chlorotic phenotype of *gr2 atm3-4* supports the interpretation that ATM3 export GSSG from mitochondria under physiological conditions. This mechanism may be important when NADPH is low, and GR2 activity limited. It should be noted, however, that toxic effects of GSSG in this case may also result from competition with other substrates of ATM3, such as persulfides as required for Fe-S cluster biosynthesis in the cytosol. In the presence of high concentrations of GSSG and with limited transport capacity in *atm3-4* these metabolites may not be exported efficiently.

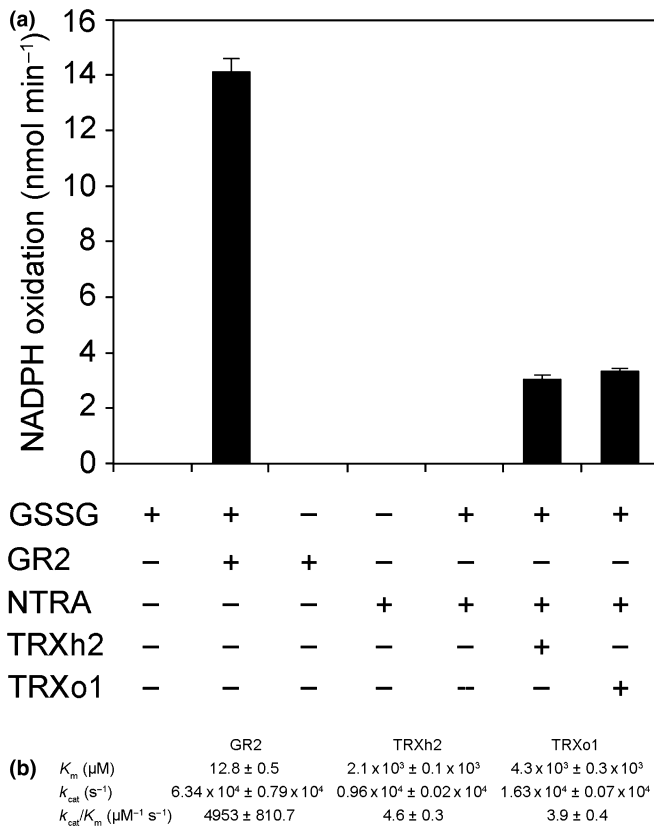


**Fig. 9** Mitochondrial TRXs in conjunction with NTRA from Arabidopsis can reduce GSSG *in vitro*. (a) Activity is monitored as NADPH oxidation. Enzymes and substrates were used at the following concentrations: NADPH, 250  $\mu\text{M}$ ; GSSG, 1 mM; GR2, 0.01  $\mu\text{M}$ ; TRXh2 and TRXo1, 2  $\mu\text{M}$ ; NTRA, 1  $\mu\text{M}$ ; Means  $\pm$  SD ( $n = 3$ ). Note that the amount of disulfide reductase protein varied between the assays. (b) Steady-state kinetic parameters of GR2 and TRX-dependent GSSG reduction systems ( $n = 3$ , means  $\pm$  SD).

Dithiol GRXs are capable of catalysing the reduction of GSSG by dihydrolipoamide (Porras *et al.*, 2002). In contrast with several nonplant species, Arabidopsis mitochondria contain only the monothiol GRXS15 which was found inactive as an oxidoreductase (Moseler *et al.*, 2015). Noncatalysed reduction of GSSG by dihydrolipoamide would be extremely inefficient and unlikely to contribute efficiently to GSSG removal. By contrast, the GSSG reduction activity of NTRs together with mitochondrial TRXs appears high enough to reduce significant amounts of GSSG. Lethality of *gr2 epc-2 ntra ntrb* shows that the situation in the mitochondrial matrix resembles the NTS-based backup of cytosolic GR1 (Marty *et al.*, 2009). The presence of multiple backup systems may explain why the lethal effect becomes apparent only after germination. In contrast to *gr2* plastids where direct detection of glutathionylated proteins, protein disulfides and further thiol modifications is not possible due to the minute amount of material in early embryos, proteomic studies in mitochondria lacking GR2 are feasible may reveal novel metabolic bottlenecks generated from oxidative modification of protein thiols and resulting imbalances in thiol switching (Nietzel *et al.*, 2019).

### Acknowledgements

This work was supported by the Deutsche Forschungsgemeinschaft (DFG) through a project grant (ME1567/3-2), the Emmy-Noether programme (SCHW1719/1-1), the priority program SPP1710 'Dynamics of thiol-based redox switches in cellular physiology' (ME1567/9-1, SCHW1719/7-1, HE 1848/16-1, WI3560/2-1) and a DAAD-Procope exchange grant to AJM and J-PR. SAKB was supported by a research fellowship of the Higher Education Council of Pakistan. Selected aspects of the work in the lab of RH/MW was supported by the DFG within the collaborative research centre 1036, TP13. This study is set within the

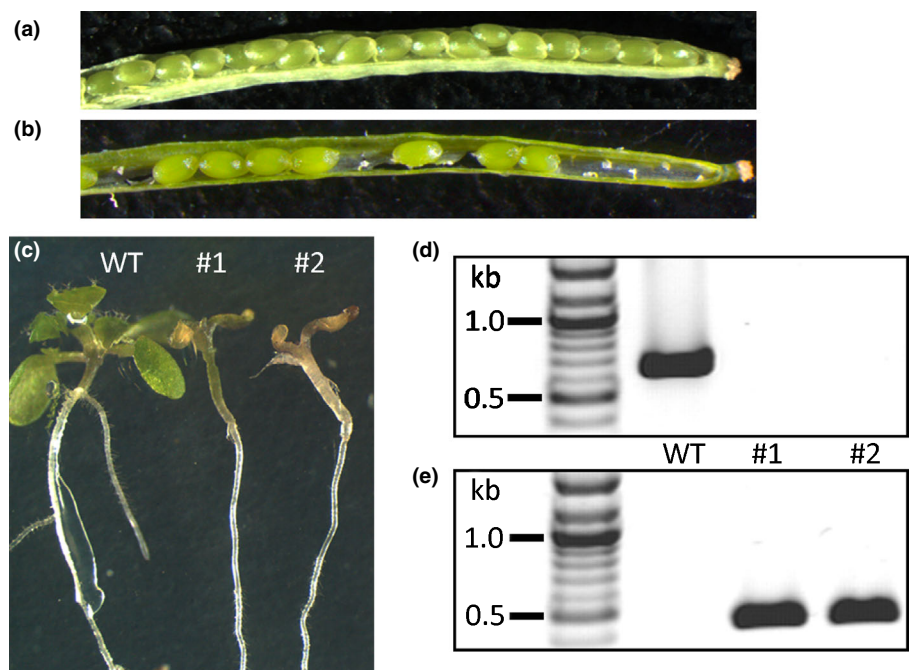


**Fig. 10** Characterization of Arabidopsis *ntra ntrb gr2* triple mutants expressing plastid-targeted GR2 under control of its endogenous promoter. (a) Wild-type (WT) silique 20 d after fertilisation. (b) Silique from a plant homozygous for both *ntra* and *gr2*, complemented with *pIGR2* and heterozygous for *ntrb*. (c) Phenotype of mutant seedlings 18 d after germination. (d, e) Genotyping of seedlings shown in panel (c) for *NTRB* (d) and the *ntrb* T-DNA insertion (e).

framework of the “Laboratoires d’Excellences (LABEX)” TULIP (ANR-10-LABX-41) and was supported in part by the Centre National de la Recherche Scientifique and by the Agence Nationale de la Recherche ANR-Blanc Cynthiol 12-BSV6-0011.

## Author contributions

AJM, RH and J-PR designed research; LM, DB, CM, SAKB, AM, MS, BZ, CR and MW performed research; JB contributed plant lines; LM, DB, CM, MS, SJM-S, J-PR and AJM analysed data and SJM-S, MS and AJM wrote the manuscript with assistance from all co-authors.

## ORCID

Janneke Balk  <https://orcid.org/0000-0003-4738-1990>  
Sajid Ali Khan Bangash  <https://orcid.org/0000-0002-6936-8060>  
Rüdiger Hell  <https://orcid.org/0000-0002-6238-4818>  
Andreas J. Meyer  <https://orcid.org/0000-0001-8144-4364>  
Anna Moseler  <https://orcid.org/0000-0003-4641-8093>  
Stefanie J. Müller-Schüssele  <https://orcid.org/0000-0003-4061-1175>  
Markus Schwarzländer  <https://orcid.org/0000-0003-0796-8308>  
Markus Wirtz  <https://orcid.org/0000-0001-7790-4022>

## References

- Albrecht SC, Sobotta MC, Bausewein D, Aller I, Hell R, Dick TP, Meyer AJ. 2014. Redesign of genetically encoded biosensors for monitoring mitochondrial redox status in a broad range of model eukaryotes. *Journal of Biomolecular Screening* 19: 379–386.
- Alexander MP. 1969. Differential staining of aborted and nonaborted pollen. *Stain Technology* 44: 117–122.
- Aller I, Rouhier N, Meyer AJ. 2013. Development of roGFP2-derived redox probes for measurement of the glutathione redox potential in the cytosol of severely glutathione-deficient *rml1* seedlings. *Frontiers in Plant Science* 4: 506.
- Alonso JM, Stepanova AN, Leisse TJ, Kim CJ, Chen H, Shinn P, Stevenson DK, Zimmerman J, Barajas P, Cheuk R *et al.* 2003. Genome-wide insertional mutagenesis of *Arabidopsis thaliana*. *Science* 301: 653–657.
- Asada K. 1999. The water–water cycle in chloroplasts: scavenging of active oxygens and dissipation of excess photons. *Annual Review of Plant Physiology and Plant Molecular Biology* 50: 601–639.
- Attacha S, Solbach D, Bela K, Moseler A, Wagner S, Schwarzländer M, Aller I, Müller SJ, Meyer AJ. 2017. Glutathione peroxidase-like enzymes cover five distinct cell compartments and membrane surfaces in *Arabidopsis thaliana*. *Plant, Cell & Environment* 40: 1281–1295.
- Begas P, Liedgens L, Moseler A, Meyer AJ, Deponte M. 2017. Glutaredoxin catalysis requires two distinct glutathione interaction sites. *Nature Communications* 8: 14835.
- Bendtsen JD, Nielsen H, von Heijne G, Brunak S. 2004. Improved prediction of signal peptides: SignalP 3.0. *Journal of Molecular Biology* 340: 783–795.
- Bernard DG, Cheng Y, Zhao Y, Balk J. 2009. An allelic mutant series of ATM3 reveals its key role in the biogenesis of cytosolic iron-sulfur proteins in *Arabidopsis*. *Plant Physiology* 151: 590–602.
- Berndt C, Hudemann C, Hanschmann E, Axelsson R, Holmgren A, Lillig C. 2007. How does iron-sulfur cluster coordination regulate the activity of human glutaredoxin 2? *Antioxidants & Redox Signaling* 9: 151–157.
- Bick JA, Aslund F, Chen Y, Leustek T. 1998. Glutaredoxin function for the carboxyl-terminal domain of the plant-type 5'-adenylylsulfate reductase. *Proceedings of the National Academy of Sciences, USA* 95: 8404–8409.
- Bryant N, Lloyd J, Sweeney C, Myoung F, Meinke D. 2011. Identification of nuclear genes encoding chloroplast-localized proteins required for embryo development in *Arabidopsis*. *Plant Physiology* 155: 1678–1689.
- Buchanan BB, Balmer Y. 2005. Redox regulation: a broadening horizon. *Annual Review of Plant Biology* 56: 187–220.
- Cairns NG, Pasternak M, Wachter A, Cobbett CS, Meyer AJ. 2006. Maturation of *Arabidopsis* seeds is dependent on glutathione biosynthesis within the embryo. *Plant Physiology* 141: 446–455.
- Chew O, Whelan J, Millar AH. 2003. Molecular definition of the ascorbate-glutathione cycle in *Arabidopsis* mitochondria reveals dual targeting of antioxidant defenses in plants. *Journal of Biological Chemistry* 278: 46869–46877.
- Clough SJ, Bent AF. 1998. Floral dip: a simplified method for *Agrobacterium*-mediated transformation of *Arabidopsis thaliana*. *The Plant Journal* 16: 735–743.
- Creissen G, Reynolds H, Xue Y, Mullineaux P. 1995. Simultaneous targeting of pea glutathione reductase and of a bacterial fusion protein to chloroplasts and mitochondria in transgenic tobacco. *The Plant Journal* 8: 167–175.
- Delorme-Hinoux V, Bangash SAK, Meyer AJ, Reichheld JP. 2016. Nuclear thiol redox systems in plants. *Plant Science* 243: 84–95.
- Dietz K-J, Pfannschmidt T. 2011. Novel regulators in photosynthetic redox control of plant metabolism and gene expression. *Plant Physiology* 155: 1477–1485.
- Ding S, Jiang R, Lu Q, Wen X, Lu C. 2016a. Glutathione reductase 2 maintains the function of photosystem II in *Arabidopsis* under excess light. *Biochimica et Biophysica Acta-Bioenergetics* 1857: 665–677.
- Ding S, Wang L, Yang Z, Lu Q, Wen X, Lu C. 2016b. Decreased glutathione reductase2 leads to early leaf senescence in *Arabidopsis*. *Journal of Integrative Plant Biology* 58: 29–47.
- Edwards K, Johnstone C, Thompson C. 1991. A simple and rapid method for the preparation of plant genomic DNA for PCR analysis. *Nucleic Acids Research* 19: 1349.
- Fahey RC. 2001. Novel thiols of prokaryotes. *Annual Review of Microbiology* 55: 333–356.
- Finkemeier I, Goodman M, Lamkemeyer P, Kandlbinder A, Sweetlove LJ, Dietz K-J. 2005. The mitochondrial type II peroxiredoxin F is essential for redox homeostasis and root growth of *Arabidopsis thaliana* under stress. *Journal of Biological Chemistry* 280: 12168–12180.
- Foyer CH, Noctor G. 2009. Redox regulation in photosynthetic organisms: signaling, acclimation, and practical implications. *Antioxidants & Redox Signaling* 11: 861–905.
- Foyer CH, Noctor G. 2011. Ascorbate and glutathione: the heart of the redox hub. *Plant Physiology* 155: 2–18.
- Fricke MD. 2016. Quantitative redox imaging software. *Antioxidants & Redox Signaling* 24: 752–762.
- Gilroy S, Białeśek M, Suzuki N, Górecka M, Devireddy AR, Karpiński S, Mittler R. 2016. ROS, calcium, and electric signals: key mediators of rapid systemic signaling in plants. *Plant Physiology* 171: 1606–1615.
- Höfgen R, Willmitzer L. 1990. Biochemical and genetic analysis of different patatin isoforms expressed in various organs of potato (*Solanum tuberosum* L.). *Plant Science* 99: 221–230.
- Ito J, Heazlewood JL, Millar AH. 2006. Analysis of the soluble ATP-binding proteome of plant mitochondria identifies new proteins and nucleotide triphosphate interactions within the matrix. *Journal of Proteome Research* 5: 3459–3469.
- Jeffery C. 2009. Moonlighting proteins—an update. *Molecular BioSystems* 5: 345–350.
- Katoh A, Uenohara K, Akita M, Hashimoto T. 2006. Early steps in the biosynthesis of NAD in *Arabidopsis* start with aspartate and occur in the plastid. *Plant Physiology* 141: 851–857.
- Ke J, Behal RH, Back SL, Nikolau BJ, Wurtele ES, Oliver DJ. 2000. The role of pyruvate dehydrogenase and acetyl-coenzyme a synthetase in fatty acid synthesis in developing *Arabidopsis* seeds. *Plant Physiology* 123: 497–508.
- Kispal G, Csere P, Prohl C, Lill R. 1999. The mitochondrial proteins Atm1p and Nfs1p are essential for biogenesis of cytosolic Fe/S proteins. *EMBO Journal* 18: 3981–3989.

- Koch M, Breithaupt C, Kiefersauer R, Freigang J, Huber R, Messerschmidt A. 2004. Crystal structure of protoporphyrinogen IX oxidase: a key enzyme in haem and chlorophyll biosynthesis. *EMBO Journal* 23: 1720–1728.
- Leighton J, Schatz G. 1995. An ABC transporter in the mitochondrial inner membrane is required for normal growth of yeast. *EMBO Journal* 14: 188–195.
- Li X, Ilarslan H, Brachova L, Qian HR, Li L, Che P, Wurtele ES, Nikolau BJ. 2011. Reverse-genetic analysis of the two biotin-containing subunit genes of the heteromeric acetyl-coenzyme A carboxylase in *Arabidopsis* indicates a unidirectional functional redundancy. *Plant Physiology* 155: 293–314.
- Lim B, Pasternak M, Meyer AJ, Cobbett CS. 2014. Restricting glutamylcysteine synthetase activity to the cytosol or glutathione biosynthesis to the plastid is sufficient for normal plant development and stress tolerance. *Plant Biology* 16: 58–67.
- Lutziger I, Oliver DJ. 2001. Characterization of two cDNAs encoding mitochondrial lipoamide dehydrogenase from *Arabidopsis*. *Plant Physiology* 127: 615–623.
- Mansfield SG, Briarty LG. 1991. Early embryogenesis in *Arabidopsis thaliana*. II. The developing embryo. *Canadian Journal of Botany* 69: 461–476.
- Marchal C, Delorme-Hinoux V, Bariat L, Siala W, Belin C, Saez-Vasquez J, Riondet C, Reichheld JP. 2014. NTR/NRX define a new thioredoxin system in the nucleus of *Arabidopsis thaliana* cells. *Molecular Plant* 7: 30–44.
- Marty L, Siala W, Schwarzländer M, Fricker MD, Wirtz M, Sweetlove LJ, Meyer Y, Meyer AJ, Reichheld J-P, Hell R. 2009. The NADPH-dependent thioredoxin system constitutes a functional backup for cytosolic glutathione reductase in *Arabidopsis*. *Proceedings of the National Academy of Sciences, USA* 106: 9109–9114.
- Maughan SC, Pasternak M, Cairns N, Kiddle G, Brach T, Jarvis R, Haas F, Nieuwland J, Lim B, Müller C *et al.* 2010. Plant homologs of the *Plasmodium falciparum* chloroquine-resistance transporter, PfCRT, are required for glutathione homeostasis and stress responses. *Proceedings of the National Academy of Sciences, USA* 107: 2331–2336.
- Meng L, Wong JH, Feldman LJ, Lemaux PG, Buchanan BB. 2010. A membrane-associated thioredoxin required for plant growth moves from cell to cell, suggestive of a role in intercellular communication. *Proceedings of the National Academy of Sciences, USA* 107: 3900–3905.
- Meyer AJ. 2008. The integration of glutathione homeostasis and redox signaling. *Journal of Plant Physiology* 165: 1390–1403.
- Meyer AJ, Brach T, Marty L, Kreye S, Rouhieh N, Jacquot J-P, Hell R. 2007. Redox-sensitive GFP in *Arabidopsis thaliana* is a quantitative biosensor for the redox potential of the cellular glutathione redox buffer. *The Plant Journal* 52: 973–986.
- Meyer AJ, Dick T. 2010. Fluorescent protein-based redox probes. *Antioxidants & Redox Signaling* 13: 621–650.
- Meyer AJ, Fricker MD. 2000. Direct measurement of glutathione in epidermal cells of intact *Arabidopsis* roots by two-photon laser scanning microscopy. *Journal of Microscopy* 198: 174–181.
- Meyer AJ, May MJ, Fricker M. 2001. Quantitative *in vivo* measurement of glutathione in *Arabidopsis* cells. *The Plant Journal* 27: 67–78.
- Mhamdi A, Hager J, Chaouch S, Queval G, Han Y, Taconnat L, Saindrenan P, Gouia H, Issakidis-Bourguet E, Renou J-P *et al.* 2010. *Arabidopsis* GLUTATHIONE REDUCTASE1 plays a crucial role in leaf responses to intracellular hydrogen peroxide and in ensuring appropriate gene expression through both salicylic acid and jasmonic acid signaling pathways. *Plant Physiology* 153: 1144–1160.
- Michalska J, Zauber H, Buchanan BB, Cejudo FJ, Geigenberger P. 2009. NTRC links built-in thioredoxin to light and sucrose in regulating starch synthesis in chloroplasts and amyloplasts. *Proceedings of the National Academy of Sciences, USA* 106: 9908–9913.
- Mittler R, Vanderauwera S, Gollery M, Van Breusegem F. 2004. Reactive oxygen gene network of plants. *Trends in Plant Science* 9: 490–498.
- Mochizuki N, Tanaka R, Grimm B, Masuda T, Moulin M, Smith AG, Tanaka A, Terry MJ. 2010. The cell biology of tetrapyrroles: a life and death struggle. *Trends in Plant Science* 15: 488–498.
- Moller IM. 2001. Plant mitochondria and oxidative stress: electron transport, NADPH turnover, and metabolism of reactive oxygen species. *Annual Review of Plant Physiology and Plant Molecular Biology* 52: 561–591.
- Moller IM, Jensen PE, Hansson A. 2007. Oxidative modifications to cellular components in plants. *Annual Review of Plant Biology* 58: 459–481.
- Morgan B, Ezerina D, Amoako TN, Riemer J, Seedorf M, Dick TP. 2013. Multiple glutathione disulfide removal pathways mediate cytosolic redox homeostasis. *Nature Chemical Biology* 9: 119–125.
- Moseler A, Aller I, Wagner S, Nietzel T, Przybyla-Toscano J, Mühlhoff U, Lill R, Berndt C, Rouhieh N, Schwarzländer M *et al.* 2015. The mitochondrial monothiol glutaredoxin S15 is essential for iron-sulfur protein maturation in *Arabidopsis thaliana*. *Proceedings of the National Academy of Science, USA* 112: 13735–13740.
- Müller-Schüssele SJ, Wang R, Gütle DD, Romer J, Rodriguez-Franco M, Scholz M, Lüth VM, Kopriva S, Dörmann P, Schwarzländer M *et al.* 2019. Chloroplasts require glutathione reductase to balance reactive oxygen species and maintain efficient photosynthesis. *bioRxiv*. <https://doi.org/10.1101/588442>
- Navrot N, Collin V, Gualberto J, Gelhaye E, Hirasawa M, Rey P, Knaff DB, Issakidis E, Jacquot J-P, Rouhieh N. 2006. Plant glutathione peroxidases are functional peroxiredoxins distributed in several subcellular compartments and regulated during biotic and abiotic stresses. *Plant Physiology* 142: 1364–1379.
- Nietzel T, Mostertz J, Ruberti C, Wagner S, Moseler A, Fuchs P, Müller-Schüssele SJ, Benamar A, Poschet G, Büttner M *et al.* 2019. Redox-mediated kick-start of mitochondrial energy metabolism drives resource-efficient seed germination. *bioRxiv*: 676213.
- Pasternak M, Lim B, Wirtz M, Hell R, Cobbett CS, Meyer AJ. 2008. Restricting glutathione biosynthesis to the cytosol is sufficient for normal plant development. *The Plant Journal* 53: 999–1012.
- Peltier J-B, Cai Y, Sun Q, Zabrouskov V, Giacomelli L, Rudella A, Ytterberg AJ, Rutschow H, van Wijk KJ. 2006. The oligomeric stromal proteome of *Arabidopsis thaliana* chloroplasts. *Molecular and Cellular Proteomics* 5: 114–133.
- Perez-Ruiz JM, Naranjo B, Ojeda V, Guinea M, Cejudo FJ. 2017. NTRC-dependent redox balance of 2-Cys peroxiredoxins is needed for optimal function of the photosynthetic apparatus. *Proceedings of the National Academy of Sciences, USA* 114: 12069–12074.
- Porras P, Pedrajas J, Martinez-Galisteo E, Padilla C, Johansson C, Holmgren A, Barceña J. 2002. Glutaredoxins catalyze the reduction of glutathione by dihydrolipoamide with high efficiency. *Biochemical and Biophysical Research Communications* 295: 1046–1051.
- Reichheld J-P, Khafif M, Riondet C, Droux M, Bonnard G, Meyer Y. 2007. Inactivation of thioredoxin reductases reveals a complex interplay between thioredoxin and glutathione pathways in *Arabidopsis* development. *Plant Cell* 19: 1851–1865.
- Reichheld J, Meyer E, Khafif M, Bonnard G, Meyer Y. 2005. AtNTRB is the major mitochondrial thioredoxin reductase in *Arabidopsis thaliana*. *FEBS Letters* 579: 337–342.
- Reumann S, Babujee L, Ma C, Wienkoop S, Siemsen T, Antonicelli GE, Rasche N, Luder F, Weckwerth W, Jahn O. 2007. Proteome analysis of *Arabidopsis* leaf peroxisomes reveals novel targeting peptides, metabolic pathways, and defense mechanisms. *Plant Cell* 19: 3170–3193.
- Sambrook J, Fritsch EF, Maniatis T. 1989. *Molecular cloning: a laboratory manual*. New York, NY, USA: Cold Spring Harbour Laboratory Press.
- Sang Y, Locy RD, Goertzen LR, Rashotte AM, Si Y, Kang K, Singh NK. 2011. Expression, *in vivo* localization and phylogenetic analysis of a pyridoxine 5'-phosphate oxidase in *Arabidopsis thaliana*. *Plant Physiology and Biochemistry* 49: 88–95.
- Sasaki Y, Nagano Y. 2004. Plant acetyl-CoA carboxylase: structure, biosynthesis, regulation, and gene manipulation for plant breeding. *Bioscience, Biotechnology and Biochemistry* 68: 1175–1184.
- Schaedler TA, Thornton JD, Kruse I, Schwarzländer M, Meyer AJ, van Veen HW, Balk J. 2014. A conserved mitochondrial ATP-binding cassette transporter exports glutathione polysulfide for cytosolic metal cofactor assembly. *Journal of Biological Chemistry* 289: 23264–23274.
- Schwarzländer M, Dick TP, Meyer AJ, Morgan B. 2016. Dissecting redox biology using fluorescent protein sensors. *Antioxidants & Redox Signaling* 24: 680–712.

- Schwarzländer M, Fricker M, Müller C, Marty L, Brach T, Novak T, Sweetlove L, Hell R, Meyer A. 2008. Confocal imaging of glutathione redox potential in living plant cells. *Journal of Microscopy* 231: 299–316.
- Serrato AJ, Perez-Ruiz JM, Spinola MC, Cejudo FJ. 2004. A novel NADPH thioredoxin reductase, localized in the chloroplast, which deficiency causes hypersensitivity to abiotic stress in *Arabidopsis thaliana*. *Journal of Biological Chemistry* 279: 43821–43827.
- Srinivasan V, Pierik AJ, Lill R. 2014. Crystal structures of nucleotide-free and glutathione-bound mitochondrial ABC transporter Atm1. *Science* 343: 1137–1140.
- Sweetlove L, Taylor N, Leaver C. 2007. Isolation of intact, functional mitochondria from the model plant *Arabidopsis thaliana*. *Methods in Molecular Biology* 372: 125–136.
- Tzafirir I, Pena-Muralla R, Dickerman A, Berg M, Rogers R, Hutchens S, Sweeney TC, McElver J, Aux G, Patton D *et al.* 2004. Identification of genes required for embryo development in *Arabidopsis*. *Plant Physiology* 135: 1206–1220.
- Veech RL, Eggleston LV, Krebs HA. 1969. The redox state of free nicotinamide-adenine dinucleotide phosphate in the cytoplasm of rat liver. *Biochemical Journal* 115: 609–619.
- Vernoux T, Wilson RC, Seeley KA, Reichheld JP, Muroy S, Brown S, Maughan SC, Cobbett CS, Van Montagu M, Inze D *et al.* 2000. The ROOT MERISTEMLESS1/CADMIUM SENSITIVE2 gene defines a glutathione-dependent pathway involved in initiation and maintenance of cell division during postembryonic root development. *Plant Cell* 12: 97–110.
- Waszczak C, Carmody M, Kangasjarvi J. 2018. Reactive oxygen species in plant signaling. *Annual Review of Plant Biology* 69: 209–236.
- Wirtz M, Hell R. 2003. Production of cysteine for bacterial and plant biotechnology: application of cysteine feedback-insensitive isoforms of serine acetyltransferase. *Amino Acids* 24: 195–203.
- Xu L, Carrie C, Law SR, Murcha MW, Whelan J. 2013. Acquisition, conservation, and loss of dual-targeted proteins in land plants. *Plant Physiology* 161: 644–662.
- Yoshida K, Hisabori T. 2016. Adenine nucleotide-dependent and redox-independent control of mitochondrial malate dehydrogenase activity in *Arabidopsis thaliana*. *Biochimica et Biophysica Acta (BBA) – Bioenergetics* 1857: 810–818.
- Yu X, Pasternak T, Eiblmeier M, Ditengou F, Kochersperger P, Sun J, Wang H, Rennenberg H, Teale W, Paponov I *et al.* 2013. Plastid-localized glutathione reductase2-regulated glutathione redox status is essential for *Arabidopsis* root apical meristem maintenance. *Plant Cell* 25: 4451–4468.
- Zannini F, Moseler A, Bchini R, Dhalleine T, Meyer AJ, Rouhier N, Couturier J. 2019. The thioredoxin-mediated recycling of *Arabidopsis thaliana* GRXS16 relies on a conserved C-terminal cysteine. *Biochimica et Biophysica Acta (BBA) – General Subjects* 1863: 426–436.

## Supporting Information

Additional Supporting Information may be found online in the Supporting Information section at the end of the article.

**Fig. S1** Schematic representation of constructs used to confirm signal peptide functionality and for compartment-specific complementation of *gr2* mutants.

**Fig. S2** Characterisation of transgenic *Arabidopsis* lines overexpressing plastid-targeted GR2.

**Fig. S3** Protein gel blot analysis of GR1 and GR2 in mitochondrial preparations of wild-type and plastid-complemented *gr2* (*epc-2*).

**Fig. S4** Characterisation of *gr2 rml1* double mutants.

**Fig. S5** High expression of SHMT<sub>TP-roGFP2</sub>-Grx1 results in incomplete mitochondrial targeting.

**Fig. S6** Mitochondrial thioredoxins reduce GSSG *in vitro* with electrons provided by NTRA and NTRB with similar efficiencies.

**Fig. S7** Crossing scheme for generation of *gr2 ntra ntrb*.

**Fig. S8** Viability stain of pollen from *ntra*<sup>-1-</sup> *gr2*<sup>-1-</sup> *NTRB/ntrb plGR2* plants.

**Methods S1** Antibody production and gel blot analysis.

**Methods S2** Immunogold labelling and electron microscopy.

**Table S1** Oligonucleotides used in this study.

**Table S2** Genetic complementation of the *gr2* mutant with compartment-specific *GR2* constructs.

**Table S3** Reciprocal cross between *ntra/ntra NTRB/ntrb gr2/gr2 plGR2* and wild-type.

Please note: Wiley Blackwell are not responsible for the content or functionality of any Supporting Information supplied by the authors. Any queries (other than missing material) should be directed to the *New Phytologist* Central Office.